

Reply to comments on “Simulating ozone dry deposition at a boreal forest with a multi-layer canopy deposition model”

October 6, 2016

We would like to appreciate the reviewer for the detailed and valuable comments which helped us a lot to improve the manuscript. Our reply to all the comments are shown below.

1. **Comments:** (1) Authors state that they have implemented a multi-layer dry deposition model into SOSAA, which is a 1D chemical transport model. SOSAA is described in Section 2.3.1, which lists different modules and references but does not explain the model types or physical principles. The key elements of SOSAA relevant to the present study, especially turbulent mixing and the derivation of eddy diffusivity, should be described in more detail.

Answer: We added a description of the turbulent mixing calculation in SOSAA and more details about the emission and chemistry as:

“In SOSAA, the horizontal wind velocity (u and v), temperature (T), specific humidity (q_v), turbulent kinetic energy (TKE) and the specific dissipation of TKE (ω) are computed every time step (10 s) by prognostic equations. In order to represent the local to synoptic scale effects, u , v , T and q_v near and within the canopy are nudged to local measurement data at SMEAR II station with a nudging factor of 0.01. A TKE- ω parameterization scheme is used to calculate the turbulent diffusion coefficients (K_t) (Sogachev, 2009),

$$K_t = C_\mu \frac{\text{TKE}}{\omega} \quad (1)$$

$$\omega = \frac{\varepsilon}{\text{TKE}} \quad (2)$$

where ε is the dissipation rate of TKE and C_μ is a closure constant. Hence the turbulent flux of a quantity X ($F_{t,X}$) can be computed as

$$F_{t,X} = -K_t \frac{\partial X}{\partial z} \quad (3)$$

where upward fluxes are positive and vice versa. Specifically, the sensible heat flux (H) and latent heat flux (LE) at each model layer are computed as

$$\text{H} = -C_{p,air} \rho_{air} K_t \left(\frac{\partial T}{\partial z} + \gamma_d \right) \quad (4)$$

$$\text{LE} = -L_v K_t \frac{\partial q_v}{\partial z} \quad (5)$$

where $C_{p,air}$ ($1009.0 \text{ J kg}^{-1} \text{ K}^{-1}$) is the specific heat capacity at constant pressure. ρ_{air} (1.205 kg m^{-3}) is the air density which is a constant in the model. γ_d (0.0098 K m^{-1}) is the lapse rate of dry air. L_v ($2.256 \times 10^6 \text{ J kg}^{-1}$) is the latent heat of vaporization for water.”

“The upper boundary values of u , v , T and q_v are constrained by the ERA-Interim reanalysis dataset provided by the European Centre for Medium-Range Weather Forecasts (ECMWF, Dee et al., 2011). At the canopy top, the incoming direct and diffuse global radiations measured at SMEAR II station, and the long wave radiation obtained from the ERA-Interim dataset are read in to improve the energy balance closure. Then the reflection, absorption, penetration and emission of three bands of radiation (long-wave, near-infrared and PAR) at each layer inside the canopy are explicitly computed according to the radiation scheme proposed by Sogachev et al. (2002). At the lower boundary, the measured soil heat flux at SMEAR II are used to further improve the representation of surface energy balance. All the input data are interpolated to match the model time for each time step. With the input data, the mass and energy exchange between atmosphere and plant cover (including the soil underneath) and the radiation attenuation inside the canopy are optimal to simulate the micrometeorological drivers of O_3 deposition at this site.”

“In current SOSAA, a modified version of MEGAN has been used to simulate the emissions of BVOCs from the trees. The emissions of some important BVOCs are included, e.g., monoterpenes (α -pinene, β -pinene, Δ^3 -carene, limonene, cineol and other minor monoterpenes (OMT)), sesquiterpenes (farnesene, β -caryophyllene and other minor sesquiterpenes (OSQ)), 2-methyl-3-buten-2-ol (MBO). The chemistry mechanism is from MCMv3.2 including needed inorganic reactions and the full MCM oxidation paths for methane (CH_4), isoprene, MBO, α -pinene, β -pinene, limonene and β -caryophyllene. We have also included the first-order oxidation reactions with OH, O_3 , NO_3 for cineole, Δ^3 -carene, OMT, farnesene and OSQ. The related chemical reactions of stabilised Criegee intermediates (sCIs) with updated reaction rates from Boy et al. (2013) are also taken into account in current simulations. For more details about emissions and chemistry we refer to Mogensen et al. (2015).”

2. **Comments: (2) Due to the incomplete model description, it is not obvious for the reader that the vertical mixing of O_3 is calculated similarly to that of any other compound in SOSAA (Eqs. 5 and 6), and that the "multi-layer O_3 deposition model" actually consists of the few resistance terms shown in Fig. 1 (of which not all are effective). As SOSAA has previously been used for simulating the exchange of reactive compounds and latent heat within a forest canopy, obviously it must include some sort of description of the surface exchange processes corresponding to stomatal uptake at least. This relationship should be explained, especially for the stomatal resistance of both overstory and understory vegetation.**

Answer:

1. As previously indicated, we added more details about the turbulent mixing which clarifies how the vertical mixing is calculated. Furthermore, we improved the prognostic equation for the evolution of the O_3 concentration for each layer and other compounds also follow this prognostic equation in SOSAA:

$$\frac{\partial[O_3]}{\partial t} = \frac{\partial}{\partial z} \left(K_t \frac{\partial[O_3]}{\partial z} \right) - V_d[O_3]A + Q_{chem} \quad (6)$$

where the first term on the right-hand side represents the vertical mixing of O_3 . The second term is the sink by dry deposition which is non-zero only inside the canopy. The last one is chemistry production and loss for O_3 for each model layer. V_d is the total dry deposition velocity at height z which already includes the uptake by the leaves, including the leaf stomata (see below), cuticle and the uptake by the soil for the understory layer. We also distinguish the difference in uptake by dry and wet leaves. A is a unit scale factor which is set to $1 \text{ m}^2 \text{ m}^{-3}$ here.

2. r_{mes} can be neglected for O_3 .
3. In SOSAA, the stomatal resistance for water vapor r_{stm,H_2O} is computed by the SCADIS module. It is used to calculate the latent heat flux and thus the energy balance. The detailed

description of the formula refers to Sogachev et al. (2002). Then r_{stm} for O_3 is obtained as

$$r_{stm} = \frac{D_{H_2O}}{D_{O_3}} r_{stm, H_2O} \quad (7)$$

Here D_{H_2O} and D_{O_3} are the molecular diffusivities of water vapor and O_3 , respectively.

3. **Comments: (3) The presentation of input data should be clearer and specify the data actually used for the deposition calculations, i.e. which data are taken from measurements and what is derived within SOSAA. This is important, as a large part of the paper is dedicated to testing the modelled meteorological variables. For example, a comparison with observations is presented for u_* , but it is not explained how the modelled profile is obtained or how it is utilised in the model.**

Answer:

1. We added more details about SOSAA description (see above) which clarifies how variables are calculated in the model. We also improved the description of the input data for the model as (this paragraph is also shown in reply 1):

“The upper boundary values of u , v , T and q_v are constrained by the ERA-Interim reanalysis dataset provided by the European Centre for Medium-Range Weather Forecasts (ECMWF, Dee et al., 2011). At the canopy top, the incoming direct and diffuse global radiations measured at SMEAR II station, and the long wave radiation obtained from the ERA-Interim dataset are read in to improve the energy balance closure. Other radiation terms are computed according to the radiation scheme in Sogachev et al. (2002). At the lower boundary, the measured soil heat flux at SMEAR II are used to further improve the representation of surface energy balance. All the input data are interpolated to match the model time for each time step. With the input data, the mass and energy exchange between atmosphere and plant cover (including the soil underneath) and the radiation attenuation inside the canopy are optimal to simulate the micrometeorological drivers of O_3 deposition at this site.”

2. u_* is calculated in SCADIS for each layer with turbulent eddy diffusivity and the wind gradient. It can represent the shear stress and thus the turbulent strength. u_* is also used to calculate the soil boundary layer resistance r_{bs} .

4. **Comments: (4.1) r_{soil} is modified from a default value based on model simulations, which are not discussed. These simulations should be shown and would serve as a useful sensitivity test.**

Answer:

1. Now we use the default value 400 s m^{-1} proposed by Ganzeveld and Lelieveld (1995) and we add a soil boundary layer resistance r_{bs} .

2. We also did a sensitivity test for r_{soil} with values of 200, 400, 600, 800 s m^{-1} . In general 400 s m^{-1} resulted in a simulation of O_3 fluxes and in-canopy concentration profiles in best agreement with observations. The analysis is added in the revised manuscript as:

“ r_{soil} varied in different studies, ranging from 10 to 180 s m^{-1} for dry soil and 180 to 1100 s m^{-1} for wet soil (Massman, 2004). In this study the dry deposition module was developed on the basis of the model from Ganzeveld and Lelieveld (1995) in which r_{soil} is 400 s m^{-1} . In order to assess the uncertainties involved in estimating r_{soil} , different values of r_{soil} ranging from 200 to 800 s m^{-1} were tested in this study (Table 1). As can be expected, the modelled O_3 fluxes decreased as r_{soil} increased. The BASE case showed the best performance in general, although it overestimated $\sim 16\%$ nighttime O_3 fluxes. Since the RSOIL200 case overestimated O_3 fluxes by $\sim 17\%$ in average for the whole month, $\sim 12\%$ at daytime and $\sim 35\%$ at nighttime, the RSOIL200 sensitivity case indicates that using this lower estimate, a value that might be more appropriate for high organic (and dry) soils, seems to not properly represent the role of

Table 1: The average and standard deviation of modelled and measured O₃ fluxes above the canopy during different time periods (ALL for the whole month, D for daytime, N for nighttime) for different cases (OBS for measurement, BASE for basic settings used in this study, RSOIL200 uses the same settings as in BASE except $r_{soil} = 200 \text{ s m}^{-1}$, similarly, RSOIL600 with $r_{soil} = 600 \text{ s m}^{-1}$ and RSOIL800 with $r_{soil} = 800 \text{ s m}^{-1}$) are shown. The relative error of modelled O₃ flux compared to the observation $(F_{t,mod} - F_{t,obs})/F_{t,obs}$ is also listed within the parentheses.

cases	ALL	D	N
OBS	0.125 ± 0.090	0.171 ± 0.085	0.052 ± 0.037
RSOIL200	0.146 ± 0.090 (+16.6%)	0.192 ± 0.085 (+12.3%)	0.070 ± 0.034 (+34.9%)
BASE	0.128 ± 0.079 (+1.93%)	0.168 ± 0.075 (-1.51%)	0.061 ± 0.030 (+16.1%)
RSOIL600	0.118 ± 0.075 (-5.85%)	0.156 ± 0.070 (-8.64%)	0.055 ± 0.029 (+5.07%)
RSOIL800	0.112 ± 0.072 (-10.7%)	0.148 ± 0.067 (-13.0%)	0.051 ± 0.028 (-2.28%)

soil removal at this site. On the other hand, taking higher resistance values, e.g., one of 600 or 800 s m⁻¹ seems to result in a better simulation of the role of the soil uptake at nighttime. However, considering the overall performance and better estimation of daytime O₃ fluxes, we still use 400 s m⁻¹ as the soil resistance.”

5. **Comments: (4.2) r_ac is set to a very small arbitrary value. What is the point of including a resistance of 1 s m-1 in series with a resistance of 600 s m-1?**

Answer: In our model the role of turbulent transport, represented by the term r_{ac} , exists but is ignored for this particular layer. Because it is a very small term compared to the other processes (e.g., molecular diffusion and surface uptake).

6. **Comments: (4.3) r_b depends on molecular diffusivity and wind speed (or friction velocity, p.9). Please present the formula or an exact reference.**

Answer: The applied relationship is according to Meyers (1987). The reference will be included in the revised manuscript.

7. **Comments: (4.4) r_stm is calculated from evapotranspiration rate in SOSAA. How?**

Answer: It is described in Answer of Comments (2).

8. **Comments: (4.5) r_mes, r_cut and r_ws have constant values. Where do these come from?**

Answer: They are from Ganzeveld and Lelieveld (1995). We will also add the detailed information in the revised paper.

9. **Comments: (4.6) f_wet is a function of RH, for which the authors cite a grey literature report that does not even include original data on canopy wetness. Isn't there anything more substantial available?**

Answer: We will add another reference: Wu et al. (2003).

10. **Comments: (5) An ineffective aerodynamic resistance term (r_ac) is included in series with the soil resistance (cf. Comment 4.2 above). However, a much more important term, namely the near-soil boundary layer resistance, is ignored in the model.**

Answer: We will add a soil boundary layer resistance r_{bs} in the revised manuscript as:

“The r_{bs} is the soil boundary layer resistance which is calculated as (Nemitz et al., 2000),

$$r_{bs} = \frac{Sc - \ln(\delta_0/z_*)}{\kappa u_{*g}} \quad (8)$$

Here Sc (1.07) is the Schmidt number for O_3 . κ is the von Kármán constant (0.41). $\delta_0 = D_{O_3}/(\kappa u_{*g})$ is the height above ground where the molecular diffusivity is equal to turbulent eddy diffusivity. z_* (0.1 m) is the height under which the logarithmic wind profile is assumed. u_{*g} is the friction velocity near the ground.”

11. **Comments: (6) The leaf surface resistance has a general formulation (Eq. 3) so as to represent both needle-shaped and broad leaves. This is accomplished by a scaling factor (alpha = 0.5) introduced to account for one-sided stomatal exchange on leaves. As the non-stomatal exchange takes place on both sides of such a leaf, with separate boundary layers, this scaling does not result in a correct formula for deposition on two-sided leaves. The authors describe alpha as a correction factor, so it may represent an approximation. However, this approximation should be justified.**

Answer: We thank the reviewer for pointing out this flaw in the implementation of the dry deposition scheme in SOSAA. Now we modified the scheme as:

“ r_{veg} is the leaf surface resistance which represents how O_3 finally deposits onto different parts of leaf surface (Fig. 1). It can be calculated at each layer for needle leaves as

$$r_{veg} = r_b + \frac{1}{1/(r_{stm} + r_{mes}) + (1 - f_{wet})/r_{cut} + f_{wet}/r_{ws}} \quad (9)$$

While for broad leaves, O_3 can deposit on a side without stomata or a side with stomata, hence r_{veg} is computed in a different way as

$$r_{veg} = 2 \left/ \left(\frac{1}{r_{veg1}} + \frac{1}{r_{veg2}} \right) \right. \quad (10)$$

$$r_{veg1} = r_b + \frac{1}{(1 - f_{wet})/r_{cut} + f_{wet}/r_{ws}} \quad (11)$$

$$r_{veg2} = r_b + \frac{1}{1/(r_{stm} + r_{mes}) + (1 - f_{wet})/r_{cut} + f_{wet}/r_{ws}} \quad (12)$$

Here r_b is the quasi-laminar boundary layer resistance over the leaf surface, which depends on molecular diffusivity and horizontal wind speed (Meyers, 1987).”

We found that the overall impact of this flaw is small so the initially presented results are still valid. For example, for a typical condition at daytime ($r_{stm}=2000.0 \text{ s m}^{-1}$, $f_{wet}=0.0$, $r_b=150.0 \text{ s m}^{-1}$), the new r_{veg} is about 3% larger than the old value for broad leaves.

12. **Comments: (7) The authors demonstrate that the model performs well in high humidity conditions but fails during the night-time when RH is low. As wet needle surfaces require additional parameterisations (RH dependent resistance, wet surface fraction), it is surprising that the authors do not first try to develop a parameterisation that performs well in dry conditions, i.e. in a much simpler case. Instead, they refer to simulation and measurement problems due to weak turbulence, but do not explain how these would depend on RH. If the measurement uncertainties increase with weakening turbulence and affect the model validation (and the u^* screening does not help), then this could be easily tested. As the soil resistance is given as a plausible explanation for the mismatch, it would also**

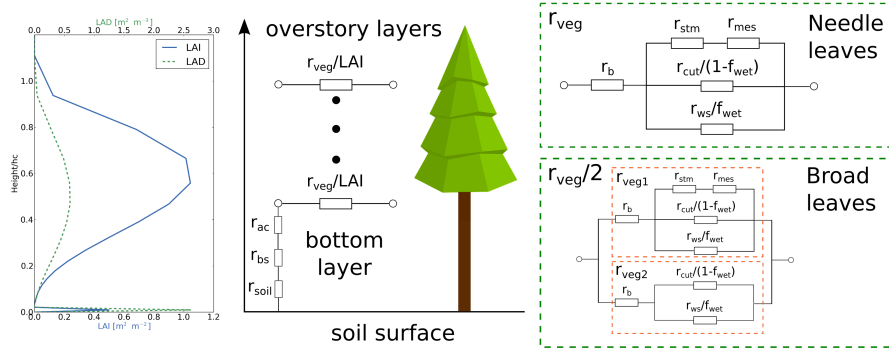


Figure 1:

seem logical to test if a better fit can be obtained by varying this resistance (see Comment 4.1. above).

Answer: This study also addresses the role of soil uptake but the reviewer is indeed correct that we didn't introduce a detailed representation of leaf/needle cuticle uptake as a function of RH. We agree with this but we also consider that there are only 69 data points under NL condition (nighttime with low humidity condition), which is a small portion compared to the total available data points of 886. This is also one reason of low correlation between the modelled and measured results for NL condition. Furthermore, the low humidity condition occurs less often at nighttime, the simulation bias for this condition only affects slightly the overall performance of the model. Therefore, we decide not yet to introduce such further modifications and rather focused on soil uptake. Further improvement on the wet skin fraction uptake will be focus of future studies with SOSAA.

13. **Comments: (8) Only ozone fluxes are considered in the analysis. As the modelled flux depends on the modelled concentration, which is affected by various processes and has a systematic diurnal cycle, it is difficult to assess how well the deposition processes are modelled by comparing fluxes alone. Perhaps you could have a look at the flux/concentration ratio (commonly called deposition velocity)?**

Answer: In this study we also compared the O_3 concentration profile in Fig. 8 which is also used to verify the model results. Therefore, the agreement between modelled and observed fluxes above the canopy and the concentration profiles inside the canopy we can conclude that the deposition processes are modelled quite well.

14. **Comments: (9) As the ozone fluxes measured at SMEAR II have been analysed in a large number of previous studies, including two different multi-layer models (Rannik et al., 2012; Launiainen et al., 2013), I would expect to see a more systematic comparison of these results. From the process modelling point of view, it would be useful to discuss how and why the modelled results differ between the three multi-layer models.**

Answer: Our study revealed some differences between our model and these two previous models, and showed the novel points of our current model by inclusion of the following statement (also see the reply below):

“Two different studies that also applied multi-layer models (Rannik et al., 2012; Launiainen et al., 2013) to simulate the O_3 fluxes and concentration inside the boreal forest canopy had their limitations on estimating the chemical contribution. Rannik et al. (2012) only considered one chemical reaction of O_3 with β -caryophyllene. In Launiainen et al. (2013), they simplified the chemical production and loss of O_3 with only two parameters to represent the first-order

kinetic sink and photo-chemical production. In this study, we implemented a chemistry module with a detailed list of chemical reactions, which was able to provide a more accurate estimation of chemical removal of O_3 inside the canopy.”

15. **Comments: (10) The discussion of chemical removal (Sect. 3.7) is based on the reactivity estimates obtained from the literature. According to the model description, the SOSAA model employed here includes a detailed chemistry module, which I assume was used in the present simulations. Why are these calculations not utilised for estimating the importance of in-canopy chemistry?**

Answer: In the revised manuscript we included the role of in-canopy chemical transformations on O_3 deposition by using the chemical module. In this way, we calculated the diurnal cycle of the net effect of chemical processes which are able to destroy O_3 by reacting with other compounds or produce O_3 by photochemical reactions. The analysis is as follows:

“In order to get rid of the effect of synoptic-scale transport of O_3 and only focus on the local sinks and sources, we implemented the case FREEO3. In this simulation case we ignored the role of advection and only considered the role of local sources and sinks inside the canopy, i.e., dry deposition, chemical production and loss, and turbulent transport. Here the time period from Aug. 5th to 14th were selected from the simulation results to analyze the local chemical contribution, because the modelled O_3 concentration fitted to the measurement the best during this period out of the whole month for the case FREEO3, which indicated that the advection only had little effect on the local observed O_3 variation. The daily averaged (from Aug. 5th to 14th) production and loss of O_3 inside the canopy caused by dry deposition (F_{depo}) and chemistry (F_{chem}) are plotted in Fig. 2. The unit $nmol\ m^2\ s^{-1}$ means that how much $nmol\ O_3$ inside the canopy alters per unit square meter per second. So positive values correspond to O_3 production and negative values represent O_3 loss. Here the chemistry production is a net effect of O_3 loss reactions and photo-chemical production. F_{depo} (obviously negative) shows a maximum O_3 loss rate at about 14:00. While the chemistry produces O_3 from morning at $\sim 06:00$ to the afternoon at $\sim 15:00$, and destroys it throughout the other moments of the day, especially at nighttime (Fig. 2). The ratio between F_{chem} and F_{depo} shows that chemical removal has its largest contribution of $\sim 9\%$ of the dry deposition sink in average at nighttime from 20:00 to 04:00. At daytime, our model simulations indicate that the O_3 production caused by chemistry can compensate up to $\sim 4\%$ of dry deposition loss in average. However, during the selected period, the chemical contribution and compensation can reach up to $\sim 24\%$ and $\sim 20\%$ at most. This indicates that in general chemistry has minor impact on O_3 alteration, but at some specific time the chemical production and removal of O_3 can still play a significant role.”

16. **Comments: (11) Even though I indicated in my access review that a linguistic revision is necessary, there are still numerous errors, some of which impair presentation. A few examples are given in the detailed comments below.**
17. **Comments: P1/L23: ”under current knowledge of air chemistry” is obvious so can be removed.**

After adding the chemistry part in our simulation, the whole paragraph:

“Furthermore, a qualitative evaluation of the chemical removal time scales indicated that the chemical removal rate within canopy was about 5% of the total deposition flux at daytime and 16% at nighttime under current knowledge of air chemistry.”

has been rewritten as:

“The chemical contribution to O_3 removal has been evaluated directly in the model simulations. According to the simulated averaged diurnal cycle the net chemical production of O_3 compensates up to $\sim 4\%$ of dry depositon loss from $\sim 06:00$ to $\sim 15:00$. During nighttime, the net chemical removal of O_3 further enhanced removal by dry deposition by a maximum \sim

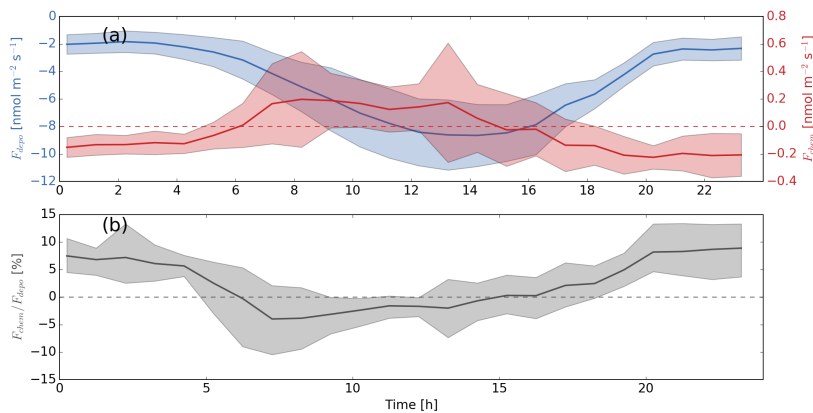


Figure 2: (a) The daily averaged (from Aug. 5th to 14th) production and loss caused by chemistry (F_{chem} , red) and dry deposition (F_{depo} , blue). (b) The ratio between F_{chem} and F_{depo} . Zero lines for F_{chem} and the ratio are plotted as dashed lines. Shaded areas show the range of ± 1 standard deviation.

9%. This indicates that there appears to be an overall relative small contribution by airborne chemical processes on O_3 removal at SMEAR II station.”

18. Comments: P2/L24: Any more recent studies?

We have not found very recent review papers focusing on the O_3 uptake on the wetness leaf surface, so we changed the statement as:

“Among them the effect of canopy wetness on O_3 deposition has attracted a lot of attention in previous studies (e.g., Massman, 2004; Altimir et al., 2006).”

19. Comments: P2/L31-: A reference is needed for ”the boreal forest emits a large portion of BVOCs”. The examples discussed are for California.

“the boreal forest emits a large portion of BVOCs”

changed to

“the boreal forest emits a large portion of BVOCs (Rinne et al., 2009)”.

20. Comments: P3/L9-12: Unclear logic. It is not only removal processes that are relevant. The introduction of eddy-covariance measurements to the discussion seems awkward. Please reformulate.

“These removal processes altogether determine the contribution of O_3 uptake on forest ground surface and understory vegetation, the vertical distribution of O_3 concentration as well as the non-stomatal uptake contribution, which are considered as three crucial challenges to understand the relationship between the eddy-covariance measurements and O_3 uptake (Launiainen et al., 2013). Therefore several numerical models ...”

changed to

“Last two decades, several numerical models ...”

21. Comments: P3/L14: Wesely (1989) describes a single model, which is based on the big-leaf approach. So this sentence (“Among these models ...”) makes little sense.

“... different climatic and environmental conditions, which are generally based on the surface deposition model described by Wesely (1989). Among these models, the so-called ”big-leaf” approach method is widely used and usually coupled to ...”

changed to

“... different climatic and environmental conditions. Many of them have implemented the big-leaf framework following the Wesely (1989) approach which can be coupled to ...”

22. **Comments: P3/L14-15, ”usually”:** Very often big-leaf models are used as inferential models.

“usually” changed to “can be”.

23. **Comments: P3/L15: Zhang et al. (2002) deal with deposition parameterisations rather than large-scale modelling.**

“e.g. Zhang et al., 2002” changed to “e.g., Hardacre et al., 2015”.

24. **Comments: P3/L18: Altimir et al. (2006) do not employ a multi-layer model.**

“e.g. Ganzeveld et al., 2002b; Altimir et al., 2006; Rannik et al., 2012; Launiainen et al., 2013” changed to

“e.g. Ganzeveld et al., 2002b; Rannik et al., 2012; Launiainen et al., 2013”

25. **Comments: P3/L23: A paper from 2000 is hardly suitable for evaluating recent models.**

We removed this sentence since it is not closely relevant to current discussion:

“Recent models have been developed more and more based on the physical, chemical and biological processes under actual environmental conditions, which reduce the dependency of empirical parameters (Wesely and Hicks, 2000).”

26. **Comments: P3/L24, ”process-based”:** Unclear which processes are referred to here. The implementation consists of a largely empirical resistance parameterisation.

“a multi-layer process-based O₃” changed to “a multi-layer O₃ ...”.

27. **Comments: P3/L33: Unclear which challenges are referred to here.**

“... for validating the new model and also shining a light on those three challenges with the model.”

changed to

“... for validating the new model and investigating more detailed processes.”

28. **Comments: P4/L23: What is meant by ”the same below”?**

It means all the height levels mentioned below are referring to above the ground level. I modified the sentence here.

“... 67.2 m (above the ground level, the same below), ...” changed to “... 67.2 m above the ground level, ...”.

29. **Comments: P4/L27-28: Why was the ozone flux calculated with data from a different anemometer than for other fluxes?**

The sensible and latent heat flux measurements were performed at a tower located at about 25 m distance from the O₃ flux measurement tower. Hence a different anemometer was used to obtain the O₃ fluxes.

30. **Comments: P4/L31: Did you correct the O3 flux data for high-frequency losses? How large were the corrections?**

Yes, sure. At this site Keronen et al. (2003) reported the correction factors 1.03–1.19 for unstable and 1.13–1.22 for stable stratification conditions (Figs. 3 and 4 in Keronen et al., 2003).

31. **Comments: P5/L28: What does "partly constrained" mean?**

"partly constrained by" changed to "constrained by".

32. **Comments: P6/L11: I would recommend against using the term "deposition velocity" for layer-specific conductances.**

We will change every layer-specific "deposition velocity" to "layer-specific conductance".

33. **Comments: P6/L19-20: What does "the unit is the same ..." mean?**

It means all the resistance shown below have the same unit "s m⁻¹". Now we removed this "the unit is the same ..." and reorganized the introduction of the resistance scheme.

34. **Comments: P6/L27-28: Unclear language; please rephrase.**

We reorganized this resistance scheme as shown in reply 11.

35. **Comments: P7/ Eq.5: This is a strange combination of partial derivatives and finite differences. Please present the equation in a mathematically consistent form. You also need to assume constant air density here. It would be more appropriate to present the 'flux' as mass flux density (g m⁻² s⁻¹).**

Answer: 1. The air density is constant in our model and we modified the prognostic equation for the simulated changes in O₃ concentration as mentioned above (reply 2):

$$\frac{\partial[\text{O}_3]}{\partial t} = \frac{\partial}{\partial z} \left(K_t \frac{\partial[\text{O}_3]}{\partial z} \right) - V_d[\text{O}_3]A + Q_{chem} \quad (13)$$

where the first term on the right-hand side represents the vertical mixing of O₃, the second term is dry deposition sink and the last one is chemistry production and loss for O₃. V_d is the total deposition velocity at height z including the vegetation and soil uptake. A is a unit scale factor which is set to 1 m² m⁻³ here.

2. This is a good suggestion. We will change the unit of flux to nmol m⁻² s⁻¹ or ng m⁻² s⁻¹, and correspondingly change O₃ concentration unit to nmol m⁻³ or ng m⁻³.

36. **Comments: P7/ Eq.5: How did you solve for [O3]. If it is a common procedure within SOSAA, perhaps you could explain it in Sect. 2.3.1.**

We explained more details in the section of SOSAA model, including a more detailed description of the calculation of turbulent mixing. All the other compounds are computed in the same way as O₃ shown here (see reply 2).

37. **Comments: P8/L1-2: How did you do the forcing? Fig. 2b does not explain this.**

We forced the O₃ concentration at 23 m to resemble the observed value every time step, the O₃ concentration at other levels are then calculated by Eq. 6. In this way, we implicitly added the role of advection in determining the surface layer (23 m) O₃ concentrations. Fig. 2b shows the gap-filled observed values which are used for the forcing.

38. **Comments: P9/Table 1: u* is not limited to the canopy top.**

"friction velocity at the canopy top" changed to "friction velocity".

39. **Comments: P9/L13, P10/L1, P11/L7, "was calculated": How? These should be moved to the methods description.**

1. We added this sentence in SOSAA description (also see reply 1):

"Then the reflection, absorption, penetration and emission of three bands of radiation (long-wave, near-infrared and PAR) at each layer inside the canopy are explicitly computed according to the radiation scheme proposed by Sogachev et al. (2002)."

2. “The PAR on top of the canopy was calculated directly from the input incoming short wave radiation with a daytime maximum of about 250–300 W m⁻² during the simulation month. Inside the canopy, PAR was calculated by considering the absorption, reflection and scattering effects of canopy leaves (Sogachev et al., 2002).”

changed to

“The PAR on top of the canopy was calculated directly from the measured incoming short wave radiation serving as input to the model, whereas PAR inside the canopy was calculated by considering the absorption, reflection and scattering effects of canopy leaves (Sogachev et al., 2002).”

3. Removed “The simulated O₃ turbulent flux was calculated from the O₃ concentration gradient and the turbulent eddy diffusivity at 23 m.” since it is explained already in the model description part.

40. Comments: P10/Fig. 2b: Gap-filling of data is not described in the paper. Why was it performed? For which variables?

Sometimes the instruments do not work or the quantities are lower than the detection limit, so we need to fill the gaps then use them as the input for the model. We will add a sentence to clarify this:

“The missing observed data points of T, RH and O₃ were gap-filled with the method described in Gierens et al. (2014).”

41. Comments: P10/L8 (also elsewhere): These data are measured well above the canopy, so why are they referred to as “canopy top”.

We think 23 m is just above the canopy and can be considered as the canopy top. We will remove these texts in section titles and change “canopy top” to “above the canopy” if necessary.

42. Comments: P11/Fig. 3, P13/Fig. 5: Are these data screened for low turbulence?

No, they included the data from the whole month, including those days with low turbulence.

43. Comments: P12/L11-12: How do the low humidity conditions affect turbulent mixing, making this difficult to simulate?

Usually at nighttime RH is larger than 70% (NH condition), under this condition, the wet skin uptake contributes more than 50% to the deposition flux, so the turbulent mixing above the ground which affects the deposition flux onto soil only plays a minor role on the deposition flux above the canopy. However, in NL condition which does not happen frequently, nearly all the deposition inside the canopy is caused by soil deposition. Hence, the difficulty of simulating the exchange processes near the surface may cause more difficulty of simulating the deposition flux into soil surface under NL condition than NH condition. Moreover, the impact of vertical advection of O₃ could be more significant in NL condition, which also complicates the analysis.

44. Comments: P13/Table 2, P15/Fig. 7: Why is the R² of the full data set higher than the R² of any of the four subsets?

This is due to the fact that the night-time observations are located close to zero, whereas daytime observations have larger absolute values but are relatively scattered. When combined, the nighttime observation improves the correlation statistics value by extending the daytime observation to zero, defining better linear relationship with improved R^2 value.

45. Comments: P14/L6: Can you estimate how much the correlation was affected by random uncertainty?

For the O₃ turbulent flux measurement at the same site Keronen et al. (2003) presented the random error statistics, defined as one standard deviation of the random uncertainty of

turbulent flux, ranging from about 10 to 40%. Such uncertainty contributed to the data scattering when comparing the modelled and measured fluxes, such as in Fig. 7, and reduced the correlation statistics. By assuming the most frequent flux relative random uncertainty value of 20%, we estimated numerically that the R^2 value is reduced by about 0.1 due to random uncertainty of flux errors. This is a rough estimate as the value depends on the distributions of the fluxes as well as their uncertainties, which are not exactly known for both measured and modelled estimates.

46. Comments: P15/Fig. 7: The caption is difficult to read.

That caption has been changed to:

“Scatter plots of modelled versus measured O_3 turbulent fluxes above the canopy. The data points are plotted separately for different groups (DH, DL, NH and NL) with their R^2 values shown in the legend. R^2 of the whole dataset is shown below the legend.”

47. Comments: P16/L11: The notation related to the cumulative flux is not obvious.

The statement on the cumulative flux calculation has been changed to:

“The normalized cumulative O_3 deposition flux at layer i can be obtained as

$$F_{c,i} = \frac{\sum_{k=1}^i F_k}{\sum_{k=1}^N F_k} \quad (14)$$

where F_k is the O_3 deposition flux at layer k and N is the layer index just above the canopy. The profiles of F_c and the contributions of different deposition pathways for four different conditions were shown in Fig. 9.”

48. Comments: P16/L14: No stomatal contribution is indicated for the understory vegetation in Figure 9.

There is $\sim 5\%$ deposition flux from stomatal uptake by the understory vegetation at daytime (Fig. 9). So we used “little contribution”.

49. Comments: P16/L14-P17/L4: Unclear presentation. Does “uptake on leaf surfaces” refer to the flux or the cumulative flux (accumulated from the bottom)?

“uptake on leaf surfaces” changed to “cumulative uptake on leaf surfaces”.

“in the NL condition when both the stomatal uptake and wet skin uptake were limited.” changed to “in the NL condition when both the cumulative stomatal uptake and wet skin uptake were limited.”

50. Comments: P17/Fig. 9: What explains the stomatal uptake during the nighttime?

Caird et al. (2007) showed that the stomata are not completely closed at night and several sources might affect the nocturnal stomatal conductance of water vapor, e.g., vapor pressure deficit, water availability (Caird et al., 2007). In SOSAA, a high value of about 13800 s m^{-1} is used for nighttime stomatal resistance of water vapor.

51. Comments: P17/L11: Please quantify the “limited O_3 uptake”, as it is obvious that small surface area corresponds to small uptake.

“providing limited O_3 uptake compared to the total O_3 deposition.” changed to “providing less than 2% O_3 uptake compared to the total O_3 deposition.”

52. Comments: P17/L12-13: These percentage contributions only refer to the mean values of the four data sets, so discussion of variation may be misleading here.

“As a result, the simulated non-stomatal contribution to the integrated O_3 deposition flux above the canopy varied from 33–56% during daytime to 85–92% during nighttime (Table 3).”

changed to

“As a result, the simulated averaged non-stomatal contribution to the integrated O₃ deposition flux above the canopy was 37% during daytime and 96% during nighttime (Table 3).”

Here we made some modifications to the resistance scheme according to the comments, so the values here are not the same as the original manuscript.

53. **Comments: P17/P13: This may be explained by Launiainen et al. (2013), but the meaning of the “sub-canopy layer” is unclear. Does it include some other vegetation surfaces in addition to the understory vegetation and soil?**

Here we used the same word “sub-canopy layer” as in Launiainen et al. (2013) to make comparison. The measurement height is 4.2 m in their research, so the sub-canopy layer here contains the understory vegetation and the soil surface below 4.2 m. No other additional vegetation is considered.

54. **Comments: P17/L14-17: The contributions cited from Launiainen et al. (2013) do not add up to 100%; why?**

35–45% is the sub-canopy layer contribution to the total O₃ deposition flux at daytime, and 25–30% is the sub-canopy layer contribution at nighttime, so they refer to the same quantity at different time periods. Therefore, they do not add up to 100%.

55. **Comments: P18/L1: How was the soil resistance determined in the first place?**

According to Ganzeveld and Lelieveld (1995) r_{soil} is 400 s m⁻¹, we also did a sensitivity test for r_{soil} and found that in general applying this global mean estimate of r_{soil} as 400 s m⁻¹ appeared to result in the best simulation of O₃ deposition fluxes and in-canopy concentrations at this site.

56. **Comments: P18/L3-5: I do not see how this conclusion about EC measurements results from the data presented here.**

The reviewer is correct, so this statement has been changed to
“Therefore, we expected that the poor performance for the NL condition also resulted from the limited data points under this condition (only 69 data points) which leads to larger ratio of random uncertainty and thus smaller R^2 .”

57. **Comments: P19/L8-9: You should explain how these percentages were obtained.**

This statement has been changed to
“These estimates showed that the chemical removal accounted for about 5% ($3384/63291 \approx 5\%$) and 16% ($9349/59880 \approx 16\%$) of the total O₃ removal within the canopy at daytime and nighttime, respectively.”

58. **Comments: P19/L24: No data on BVOC removal are presented in this study.**

We are preparing a document on the role of canopy deposition in BVOC exchange for this site. However, the reviewer is right in that we do not further present here any results on BVOC deposition and consequently the statement has been changed to
“... e.g., by the dry and wet cuticle, by stomatal uptake and by the soil surface.”

59. **Comments: P20/L14: Poor presentation; please rephrase.**

The statement has been changed to
“Our study indicates that uptake by the wet canopy appears to dominate nocturnal removal at this site with a relative smaller role of soil removal especially during high humidity conditions.”

60. **Comments: P20/L19-20: I do not see how these different flux partitionings would indicate “the difficulty of simulating and measuring O₃ deposition at night”.**
 Removed “This also indicated the difficulty of simulating and measuring O₃ deposition at night with weak turbulence (Rannik et al., 2009).”
61. **Comments: Technical comments**
62. **Comments: P1/L18,L19: Incorrect grammar.**
 “was similar to” changed to “was similar as the contribution reported in”
 “two times as” changed to “two times larger than”
63. **Comments: P2/L1-3: Unnecessary material for the abstract.**
 Removed “The evaluation of the O₃ deposition processes provides improved understanding about the mechanisms involved in the removal of O₃ for this boreal forest site which are also relevant to the removal of other reactive compounds such as the BVOCs and their oxidation products, which will be focus of a follow-up study.”
64. **Comments: P3/L27-28: “manuscript in preparation” is not a useful reference.**
 “(MLC-CHEM, manuscript in preparation).” changed to “(MLC-CHEM, e.g., Ganzeveld et al. (2002))”
65. **Comments: P5/L10: Incorrect grammar.**
 “a more strictly criteria” changed to “a more strict criteria”
66. **Comments: P8/L8: Incorrect grammar.**
 “The time series of temperature especially this transition were well predicted by the model (Fig. 2a).”
 changed to
 “Analysis of the full temperature record indicates that this transition in the weather conditions at the site was well simulated by the model.”
67. **Comments: P8/L13: Repetition from the introduction.**
 Removed “It was also interesting to study this featured time period with hot and dry climate which probably represented a future trend at this boreal forest site (Williams et al., 2011).”
68. **Comments: P9/L1 (also elsewhere): replace “showed” by “shows”.**
 “Figure 3 showed the comparison results ...” changed to “Figure 3 shows the comparison results ...”
 “Figure 3a showed the good agreement ...” changed to “Figure 3a shows the good agreement ...”
 “Figure 7 showed the correlation ...” changed to “Figure 7 shows the correlation ...”
69. **Comments: P12/L9,L13: Incorrect grammar.**
 L9: “followed by the condition DH with R^2 of 0.30, both of them were under high humidity conditions.”
 changed to
 “followed by the results reflecting the daytime high humidity conditions. Note that these conditions with highest correlations were also the conditions with high relative humidity.”
 L13: “the nighttime O₃ turbulent flux were affected by” changed to “the nighttime O₃ turbulent flux was affected by”

70. **Comments: P17/L17: Typo.**

“Tabel 3” changed to “Table 3”

71. **Comments: P20/L9: Incorrect grammar**

“were significant in the total O₃ uptake” changed to “were significant for the total O₃ uptake”

References

- Altimir, N., Kolari, P., Tuovinen, J.-P., Vesala, T., Bäck, J., Suni, T., Kulmala, M., and Hari, P. (2006). Foliage surface ozone deposition: a role for surface moisture? *Biogeosciences*, 3:209–228.
- Boy, M., Mogensen, D., Smolander, S., Zhou, L., Nieminen, T., Paasonen, P., Plass-Dülmer, C., Sipilä, M., Petäjä, T., Mauldin, L., Berresheim, H., and Kulmala, M. (2013). Oxidation of so₂ by stabilized criegee intermediate (sci) radicals as a crucial source for atmospheric sulfuric acid concentrations. *Atmospheric Chemistry and Physics*, 13(7):3865–3879.
- Caird, M. A., Richards, J. H., and Donovan, L. A. (2007). Nighttime Stomatal Conductance and Transpiration in C₃ and C₄ Plants. *Plant Physiology*, 143:4–10.
- Dee, D. P., Uppala, S. M., Simmons, A. J., Berrisford, P., Poli, P., Kobayashi, S., Andrae, U., Balmaseda, M. A., Balsamo, G., Bauer, P., Bechtold, P., Beljaars, A. C. M., van de Berg, L., Bidlot, J., Bormann, N., Delsol, C., Dragani, R., Fuentes, M., Geer, A. J., Haimberger, L., Healy, S. B., Hersbach, H., Hólm, E. V., Isaksen, I., Kållberg, P., Köhler, M., Matricardi, M., McNally, A. P., Monge-Sanz, B. M., Morcrette, J.-J., Park, B.-K., Peubey, C., de Rosnay, P., Tavolato, C., Thépaut, J.-N., and Vitart, F. (2011). The era-interim reanalysis: configuration and performance of the data assimilation system. *Quarterly Journal of the Royal Meteorological Society*, 137(656):553–597.
- Ganzeveld, L. and Lelieveld, J. (1995). Dry deposition parameterization in a chemistry general circulation model and its influence on the distribution of reactive trace gases. *J. Geophys. Res.*, 100:20999–21012.
- Ganzeveld, L. N., Lelieveld, J., Dentener, F. J., Krol, M. C., and Roelofs, G.-J. (2002). Atmosphere-biosphere trace gas exchanges simulated with a single-column model. *Journal of Geophysical Research*, 107(D16):ACH 8–1–ACH 8–21.
- Gierens, R. T., Laakso, L., Mogensen, D., Vakkari, V., Beukes, J. P., Van Zyl, P. G., Hakola, H., Guenther, A., Pienaar, J. J., and Boy, M. (2014). Modelling new particle formation events in the south african savannah. *South African Journal of Science*.
- Keronen, P., Reissell, A., Rannik, Ü., Pohja, T., Siivola, E., Hiltunen, V., Hari, P., Kulmala, M., and Vesala, T. (2003). Ozone flux measurements over a scots pine forest using eddy covariance method: performance evaluation and comparison with flux-profile method. *Boreal. Environ. Res.*, 8:425–443.
- Launiainen, S., Katul, G. G., Grönholm, T., and Vesala, T. (2013). Partitioning ozone fluxes between canopy and forest floor by measurements and a multi-layer model. *Agricultural and Forest Meteorology*, 173:85–99.
- Massman, W. J. (2004). Toward an ozone standard to protect vegetation based on effective dose: a review of deposition resistances and a possible metric. *Atmospheric Environment*, 38:2323–2337.
- Meyers, T. P. (1987). The sensitivity of modeled so₂ fluxes and profiles to stomatal and boundary layer resistances. *Water, Air, and Soil Pollution*, 35(3):261–278.

- Mogensen, D., Gierens, R., Crowley, J. N., Keronen, P., Smolander, S., Sogachev, A., Nölscher, A. C., Zhou, L., Kulmala, M., Tang, M. J., Williams, J., and Boy, M. (2015). Simulations of atmospheric OH, O₃ and NO₃ reactivities within and above the boreal forest. *Atmos. Chem. Phys.*, 15:3909–3932.
- Nemitz, E., Sutton, M. A., Schjoerring, J. K., Husted, S., and Paul, W. G. (2000). Resistance modelling of ammonia exchange over oilseed rape. *Agricultural and Forest Meteorology*, 105:405–425.
- Rannik, U., Altimir, N., Mammarella, I., Bäck, J., Rinne, J., Ruuskanen, T. M., Hari, P., Vesala, T., and Kulmala, M. (2012). Ozone deposition into a boreal forest over a decade of observations: evaluating deposition partitioning and driving variables. *Atmospheric Chemistry and Physics*, 12(24):12165–12182.
- Rinne, J., Bäck, J., and Hakola, H. (2009). Biogenic volatile organic compound emissions from the eurasian taiga: current knowledge and future directions. *Boreal Environment Research*, 14:807–826.
- Sogachev, A. (2009). A note on two-equation closure modelling of canopy flow. *Boundary-Layer Meteorol.*, 130:423–435.
- Sogachev, A., Menzhulin, G., Heimann, M., and Lloyd, J. (2002). A simple three dimensional canopy – planetary boundary layer simulation model for scalar concentrations and fluxes. *Tellus*, 54B:784–819.
- Wesely, M. L. (1989). Parameterization of surface resistances to gaseous dry deposition in regional-scale numerical models. *Atmos. Env.*, 23:1293–1304.
- Wesely, M. L. and Hicks, B. B. (2000). A review of the current status of knowledge on dry deposition. *Atmospheric Environment*, 34:2261–2282.
- Wu, Y., Brashers, B., Finkelstein, P. L., and E., P. J. (2003). A multilayer biochemical dry deposition model 1. model formulation. *Journal of Geophysical Research: Atmospheres*, 108(D1).

Reply to comments on "Simulating ozone dry deposition at a boreal forest with a multi-layer canopy deposition model"

October 6, 2016

We thank the reviewer's thoughtful comments which are helpful not only for this manuscript but also for our future research. Our reply for all the comments are shown below.

1. **Comments: 1. However, I would have appreciated a more extended parameterization and a better description of the model in order to clearly understand the formalism adopted to predict energy balance terms.**

We added more details about the energy balance terms, including sensible and latent heat fluxes, soil heat flux and radiation.

"In SOSAA, the horizontal wind velocity (u and v), temperature (T), specific humidity (q_v), turbulent kinetic energy (TKE) and the specific dissipation of TKE (ω) are computed every time step (10 s) by prognostic equations. In order to represent the local to synoptic scale effects, u , v , T and q_v near and within the canopy are nudged to local measurement data at SMEAR II station with a nudging factor of 0.01. A TKE- ω parameterization scheme is used to calculate the turbulent diffusion coefficients (K_t) (Sogachev, 2009),

$$K_t = C_\mu \frac{\text{TKE}}{\omega} \quad (1)$$

$$\omega = \frac{\varepsilon}{\text{TKE}} \quad (2)$$

where ε is the dissipation rate of TKE and C_μ is a closure constant. Hence the turbulent flux of a quantity X ($F_{t,X}$) can be computed as

$$F_{t,X} = -K_t \frac{\partial X}{\partial z} \quad (3)$$

where upward fluxes are positive and vice versa. Specifically, the sensible heat flux (H) and latent heat flux (LE) at each model layer are computed as

$$H = -C_{p,air} \rho_{air} K_t \left(\frac{\partial T}{\partial z} + \gamma_d \right) \quad (4)$$

$$LE = -L_v K_t \frac{\partial q_v}{\partial z} \quad (5)$$

where $C_{p,air}$ ($1009.0 \text{ J kg}^{-1} \text{ K}^{-1}$) is the specific heat capacity at constant pressure. ρ_{air} (1.205 kg m^{-3}) is the air density which is a constant in the model. γ_d (0.0098 K m^{-1}) is the lapse rate of dry air. L_v ($2.256 \times 10^6 \text{ J kg}^{-1}$) is the latent heat of vaporization for water."

"The upper boundary values of u , v , T and q_v are constrained by the ERA-Interim reanalysis dataset provided by the European Centre for Medium-Range Weather Forecasts (ECMWF, Dee et al., 2011). At the canopy top, the incoming direct and diffuse global radiations measured

Table 1: The average and standard deviation of modelled and measured (OBS) O₃ fluxes above the canopy for different conditions in different cases are shown. The relative change of modelled O₃ flux compared to the observation $(F_{t,mod} - F_{t,obs})/F_{t,obs}$ is also listed within the parentheses.

cases	ALL	D	N
OBS	0.125 ± 0.090	0.171 ± 0.085	0.052 ± 0.037
RSOIL200	0.146 ± 0.090 (+16.6%)	0.192 ± 0.085 (+12.3%)	0.070 ± 0.034 (+34.9%)
BASE	0.128 ± 0.079 (+1.93%)	0.168 ± 0.075 (-1.51%)	0.061 ± 0.030 (+16.1%)
RSOIL600	0.118 ± 0.075 (-5.85%)	0.156 ± 0.070 (-8.64%)	0.055 ± 0.029 (+5.07%)
RSOIL800	0.112 ± 0.072 (-10.7%)	0.148 ± 0.067 (-13.0%)	0.051 ± 0.028 (-2.28%)

at SMEAR II station, and the long wave radiation obtained from the ERA-Interim dataset are read in to improve the energy balance closure. Then the reflection, absorption, penetration and emission of three bands of radiation (long-wave, near-infrared and PAR) at each layer inside the canopy are explicitly computed according to the radiation scheme proposed by Sogachev et al. (2002). At the lower boundary, the measured soil heat flux at SMEAR II are used to further improve the representation of surface energy balance. All the input data are interpolated to match the model time for each time step. With the input data, the mass and energy exchange between atmosphere and plant cover (including the soil underneath) and the radiation attenuation inside the canopy are optimal to simulate the micrometeorological drivers of O₃ deposition at this site.”

2. **Comments: 2. There are some arbitrary choices of parameters, and not a convincing analysis of sensitivity or results from a model calibration. A table showing results from a sensitivity analysis should be provided.**

We added a sensitivity test of r_{soil} as below:

“ r_{soil} varied in different studies, ranging from 10 to 180 s m⁻¹ for dry soil and 180 to 1100 s m⁻¹ for wet soil (Massman, 2004). In this study the dry deposition module was developed on the basis of the model from Ganzeveld and Lelieveld (1995) in which r_{soil} is 400 s m⁻¹. In order to assess the uncertainties involved in estimating r_{soil} , different values of r_{soil} ranging from 200 to 800 s m⁻¹ were tested in this study (Table 1). As can be expected, the modelled O₃ fluxes decreased as r_{soil} increased. The BASE case showed the best performance in general, although it overestimated ~ 16% nighttime O₃ fluxes. Since the RSOIL200 case overestimated O₃ fluxes by ~ 17% in average for the whole month, ~ 12% at daytime and ~ 35% at nighttime, the RSOIL200 sensitivity case indicates that using this lower estimate, a value that might be more appropriate for high organic (and dry) soils, seems to not properly represent the role of soil removal at this site. On the other hand, taking higher resistance values, e.g., one of 600 or 800 s m⁻¹ seems to result in a better simulation of the role of the soil uptake at nighttime. However, considering the overall performance and better estimation of daytime O₃ fluxes, we still use 400 s m⁻¹ as the soil resistance.”

3. **Comments: 3. Basic questions like: what could be the effect of an increase in air temperature and precipitation regimes on ozone deposition? Are not resolved, although it would have been nice triggering the model for some predictions of Ozone deposition under future environmental changes. In general the paper lacks of more mechanistic explanations of the results, with more discussion on the possible drivers of dry and wet ozone deposition.**

The reviewer has a point also since we have indicated that the observational dataset included data that were potentially resembling more common future conditions at this boreal forest site. However, in the present study we decided to limit ourselves to analyse the model performance

for the contrasting day and night time, wet and dry conditions to evaluate the role of the various substrates in the overall O_3 removal. This also reveals the potential significance of non-stomatal removal mechanisms at this site which calls for a better representation of these processes. Such a further improved model could then be applied in follow-up studies to assess what future climate change conditions could imply for removal of pollutants such as O_3 but also other related compounds over boreal forests.

4. **Comments: 4. Pag 2 line 25: You mention again that dew on leaves can increase deposition, but could you spend two lines mentioning the reasons or hypothesis why a hydrophobic molecule reacts so fast on wet surfaces?**

We added this description in the introduction:

“Previous studies showed that both the micro structure of the leaf surface and the hydrophilic compounds existing on the leaf surface are able to facilitate the formation of the water films or clusters, although the foliage surface itself is hydrophobic (Altimir et al., 2006). As a result, the different dissolved compounds like organics in the solution formed on leaf surface could react with O_3 and thus enhance the O_3 uptake (Altimir et al., 2006).”

5. **Comments: 5. Pag 3 line 10. What about NO_x emitted from soils? Couldn't fast reactions between O₃ and NO lead to high O₃ fluxes in the sub-canopy region?**

In SMEAR II station, NO emission is about $6 \text{ ng(N) m}^{-2} \text{ h}^{-1}$ which is close to the detection limit (Pilegaard et al., 2006). Moreover, according to the results in Rannik et al. (2009), the O_3 uptake due to reaction with NO emission is only about 0.0025% ($10^{-4} \text{ nmol m}^{-2} \text{ s}^{-1} / 4 \text{ nmol m}^{-2} \text{ s}^{-1}$) of the total nighttime O_3 flux. The sub-canopy O_3 flux at nighttime was about 25–30% of total O_3 uptake, so the effect of reaction with NO on sub-canopy O_3 flux can be ignored.

6. **Comments: 6. Pag 3 line 34: Only one month to test the model? The relative contributions of O₃ sinks changes a lot during the seasons in response to air temperature and plant phenology. It is a pity that such an important modelling effort is limited to one month, I would extend to the all vegetative season.**

It would indeed be nice to conduct an analysis of a full seasonal cycle but this month was giving access to a complete dataset giving the best constraints for the presented detailed evaluation of the model also having still quite some large contrasts. Moreover, first assessing a proper representation of the main drivers of O_3 exchange would then also allow use of the model for full seasonal cycle studies in future research.

7. **Comments: 7. Pag 5 line 5: Extensive research has been conducted in Yuttiala to refine turbulence limitation to flux measurements. Why should we expect an ustar threshold different from other scalars measured at the site?**

Different scalars may be differently affected by the nighttime phenomena such as accumulation, vertical as well as horizontal advection and in more general by stability conditions. This is due to build up of the concentration gradient which is expected to be particularly large for emitted compounds such as carbon dioxide. Ozone is instead deposited and therefore no large concentration gradients can form, meaning also that the mass balance components other than vertical transport are expected to be smaller. We use the criterion velocity threshold well justified for O_3 e.g. by Rannik et al. (2009).

8. **Comments: 8. Pag 6 line 20: do you have experience of subcanopy O₃ fluxes so that you can better parameterize soil resistances? It seems here that usage of one value rather than another is arbitrary and not properly calibrated.**

The process of O_3 uptake by soil includes understorey transport (r_{ac}), diffusion at the soil/litter layer interface (r_{bs}) and, finally uptake by this soil/litter layer (r_{soil}) which might be strongly

affected by wetness. In this study we ignored r_{ac} since the height of the lowest layer is only about 0.3 m above the ground where vertical transport is mainly limited by the molecular diffusion above the surface which is represented by r_{bs} . r_{bs} will be added in the revised manuscript as:

“The r_{bs} is the soil boundary layer resistance which is calculated as (Nemitz et al., 2000),

$$r_{bs} = \frac{Sc - \ln(\delta_0/z_*)}{\kappa u_{*g}} \quad (6)$$

Here Sc (1.07) is the Schmidt number for O_3 . κ is the von Kármán constant (0.41). $\delta_0 = D_{O_3}/(\kappa u_{*g})$ is the height above ground where the molecular diffusivity is equal to turbulent eddy diffusivity. z_* (0.1 m) is the height under which the logarithmic wind profile is assumed. u_{*g} is the friction velocity near the ground.”

For the soil/litter layer resistance r_{soil} , we are aware that application of the value 400 s m^{-1} deemed to represent the global mean soil uptake efficiency and is thus a very crude simplification. However, from the conducted sensitivity analysis it can be inferred that this crude representation appears to result in the best representation of both O_3 deposition fluxes as well as O_3 concentration profiles inside the canopy. Actual confirmation of the correctness of the selected value can only be done conducting more detailed soil uptake measurements. Our study also clearly demonstrates the need for such additional measurements.

9. **Comments: 9. Pag 7 line 15. So you mean that K_t has been estimated from measured fluxes? Or in which other way? Reading through the manuscript I feel like the description of the model is not accurate, and more informations should be provided.**

We added more detailed description about the model SOSAA as described above. So K_t is calculated in the model from a TKE- ω scheme.

10. **Comments: 10. Pag 19 line 15: Can you say that NOx are also not relevant in the boreal forest?**

Yes, from previous studies, we can conclude that NOx is not relevant to the O_3 uptake in SMEAR II station as we discussed above: At the SMEAR II station, NO emission is close to the detection limit (Pilegaard et al., 2006) and the O_3 uptake due to reaction with NO can be ignored (Rannik et al., 2009).

11. **Comments: 11. Pag 20 line 11: Since the Stomatal resistance is calculated based on evapotranspiration, are you sure that relevant nocturnal soil evaporation does not contribute significantly to R_c ? Have you tried to separate canopy transpiration from soil evaporation in the model?**

Actaully, the stomatal resistance is calculated based on the evapotranspiration from leaves and is already separated from soil evaporation in the model. Therefore, the soil evaporation does not contribute to stomatal conductance in the model.

References

- Altimir, N., Kolari, P., Tuovinen, J.-P., Vesala, T., Bäck, J., Suni, T., Kulmala, M., and Hari, P. (2006). Foliage surface ozone deposition: a role for surface moisture? *Biogeosciences*, 3:209–228.
- Dee, D. P., Uppala, S. M., Simmons, A. J., Berrisford, P., Poli, P., Kobayashi, S., Andrae, U., Balmaseda, M. A., Balsamo, G., Bauer, P., Bechtold, P., Beljaars, A. C. M., van de Berg, L., Bidlot, J., Bormann, N., Delsol, C., Dragani, R., Fuentes, M., Geer, A. J., Haimberger, L., Healy, S. B., Hersbach, H., Hólm, E. V., Isaksen, I., Kållberg, P., Köhler, M., Matricardi, M.,

- McNally, A. P., Monge-Sanz, B. M., Morcrette, J.-J., Park, B.-K., Peubey, C., de Rosnay, P., Tavolato, C., Thépaut, J.-N., and Vitart, F. (2011). The era-interim reanalysis: configuration and performance of the data assimilation system. *Quarterly Journal of the Royal Meteorological Society*, 137(656):553–597.
- Ganzeveld, L. and Lelieveld, J. (1995). Dry deposition parameterization in a chemistry general circulation model and its influence on the distribution of reactive trace gases. *J. Geophys. Res.*, 100:20999–21012.
- Massman, W. J. (2004). Toward an ozone standard to protect vegetation based on effective dose: a review of deposition resistances and a possible metric. *Atmospheric Environment*, 38:2323–2337.
- Nemitz, E., Sutton, M. A., Schjoerring, J. K., Husted, S., and Paul, W. G. (2000). Resistance modelling of ammonia exchange over oilseed rape. *Agricultural and Forest Meteorology*, 105:405–425.
- Pilegaard, K., Skiba, U., Ambus, P., Beier, C., Brüggemann, N., Butterbach-Bahl, K., Dick, J., Dorsey, J., Duyzer, J., Gallagher, M., Gasche, R., Horvath, L., Kitzler, B., Leip, A., Pihlatie, M. K., Rosenkranz, P., Seufert, G., Vesala, T., Westrate, H., and Zechmeister-Boltenstern, S. (2006). Factors controlling regional differences in forest soil emission of nitrogen oxides (NO and N₂O). *Biogeosciences*, 3(4):651–661.
- Rannik, U., Mammarella, I., Keronen, P., and Vesala, T. (2009). Vertical advection and nocturnal deposition of ozone over a boreal pine forest. *Atmospheric Chemistry and Physics*, 9(6):2089–2095.
- Sogachev, A. (2009). A note on two-equation closure modelling of canopy flow. *Boundary-Layer Meteorol.*, 130:423–435.
- Sogachev, A., Menzhulin, G., Heimann, M., and Lloyd, J. (2002). A simple three dimensional canopy – planetary boundary layer simulation model for scalar concentrations and fluxes. *Tellus*, 54B:784–819.

Simulating ozone dry deposition at a boreal forest with a multi-layer canopy deposition model

Putian Zhou¹, Laurens Ganzeveld², Üllar Rannik¹, Luxi Zhou^{1, *}, Rosa Gierens^{1, **}, Ditte Taipale^{3,4}, Ivan Mammarella¹, and Michael Boy¹

¹University of Helsinki, Department of Physics, P.O. Box 64, FI-00014, University of Helsinki, Finland

²~~Wageningen-UR~~ Meteorology and Air Quality (MAQ), Department of Environmental Sciences, Wageningen University and Research Centre, Wageningen, Netherlands

³University of Helsinki, Department of Forest Sciences, P.O. Box 27, FI-00014, University of Helsinki, Finland

⁴Estonian University of Life Sciences, Department of Plant Physiology, Kreutzwaldi 1, EE-51014, Estonia

* now at U.S. Environmental Protection Agency, Research Triangle Park, NC, USA

** now at Institute for Geophysics and Meteorology, University of Cologne, Germany

Correspondence to: Zhou Putian (putian.zhou@helsinki.fi)

Abstract. A multi-layer ozone (O₃) dry deposition model has been implemented into SOSAA (a model to Simulate the concentrations of Organic vapours, Sulphuric Acid and Aerosols) to improve the representation of O₃ concentration and flux within and above the forest canopy in the planetary boundary layer. We aim to predict the O₃ uptake by a boreal forest canopy under varying environmental conditions and analyse the influence of different factors on total O₃ uptake by the canopy as well as the vertical distribution of deposition sinks inside the canopy. We evaluated the newly implemented canopy dry deposition model was validated by an extensive comparison of simulated and observed O₃ turbulent fluxes and concentration profiles within and above the boreal forest canopy at SMEAR II (the Station to Measure Ecosystem-Atmosphere Relation II) in Hyytiälä, Finland, in August, 2010.

~~The first half of August showed extremely warm and dry conditions which were probably representative for summer conditions prevailing at this site in future. The simulated O₃ turbulent fluxes at the canopy top and the O₃ concentration profiles inside the canopy agreed well with the measurement, which indicated that the turbulent transport and the O₃ dry deposition onto the canopy and soil surface appeared to be properly represented in the model.~~

In this model, the fraction of wet surface on vegetation leaves was parameterised according to the ambient relative humidity (RH). Model results showed that when RH was larger than 70% the O₃ uptake onto wet skin contributed 48.6~ 51% to the total deposition during nighttime and 22.0~ 19% during daytime. In addition, most of the O₃ deposition occurred below 0.8 h_c (canopy height) at this site. The contribution of sub-canopy deposition below 4.2 m was modelled to be about 40% of the total O₃ deposition during daytime which was similar to previous studies. Whereas for nighttime, the simulated sub-canopy deposition contributed 40–65% to the total O₃ deposition which was about two times as that in previous studies (25–30%). The overall contribution of soil uptake was estimated as 36.5%. These results indicated the importance of non-stomatal O₃ uptake processes, especially the uptake on wet skin and soil surface.

Furthermore, a qualitative evaluation of the chemical removal time scales indicated that the chemical removal rate within canopy was about 5% of the total deposition flux at daytime and 16% at nighttime under current knowledge of air chemistry.

The evaluation of the O₃ deposition processes provides improved understanding about the mechanisms involved in the removal of O₃ for this boreal forest site which are also relevant to the removal of other reactive compounds such as the BVOCs and their oxidation products, which will be focus of a follow-up study. And the overall contribution of soil uptake was estimated about 36%. The contribution of sub-canopy deposition below 4.2 m was modelled to be ~ 38% of the total O₃ deposition during daytime which was similar to the contribution reported in previous studies. The chemical contribution to O₃ removal was evaluated directly in the model simulations. According to the simulated averaged diurnal cycle the net chemical production of O₃ compensated up to ~ 4% of dry deposition loss from about 06:00 to 15:00. During nighttime, the net chemical loss of O₃ further enhanced removal by dry deposition by a maximum ~ 9%. Thus the results indicated that an overall relatively small contribution by airborne chemical processes to O₃ removal at this site.

10 1 Introduction

Tropospheric ozone (O₃) is an important oxidant of many reactive species such as biogenic volatile organic compounds (BVOCs) emitted from the forest canopy (Bäck et al., 2012; Smolander et al., 2014). It also plays a significant role in the regulation of the atmospheric oxidation capacity first of all by being one of the primary sources of the hydroxyl radical (OH) which is the most critical oxidant in the air (Mogensen et al., 2015). O₃ also initiates the formation of Criegee intermediate (CI) radicals which are crucial in tropospheric oxidation (Boy et al., 2013). As an air pollutant, O₃ can cause damage to human health (Kampa and Castanas, 2008) and affect ecosystem functioning via its various toxic impacts (Felzer et al., 2007). O₃ can also alter the global radiative forcing as an important greenhouse gas (Stocker et al., 2013, chap. 2). Hence it is important to understand the O₃ budget including its sources and sinks at local or site scale in order to understand the global scale implications.

O₃ is produced via photochemical reactions in the presence of precursor gases, e.g., volatile organic compounds (VOCs), CO (carbon oxide), OH and NO_x (nitric oxide and nitrogen dioxide) or transported downward from stratosphere, and is removed mainly near the Earth's surface. For vegetated surfaces a large part of the removal processes are via stomatal uptake on leaf surface and non-stomatal uptake on plant canopies and soil surface (Wesely, 1989; Ganzeveld and Lelieveld, 1995; Altimir et al., 2006; Rannik et al., 2012; Launiainen et al., 2013), as well as depleted by chemical reactions (Kurpius and Goldstein, 2003; Wolfe et al., 2011). In this study we **only** focus on the O₃ removal **and production** processes **within and immediately above the canopy**, more particularly on the O₃ uptake by boreal forest which covers 33% of global forest land (Ruckstuhl et al., 2008).

For vegetation, the uptake of O₃ depends on the turbulence intensity above and within the canopy, the diffusive transfer in the quasi-laminar boundary layer over the leaf surface, the biological properties of the plants, surface wetness condition, and soil type (Ganzeveld and Lelieveld, 1995). Among them the effect of canopy wetness on O₃ deposition has attracted a lot of attention in previous studies ~~which were also summarised in Massman (2004)~~ (e.g., Massman, 2004; Altimir et al., 2006). For different vegetation types and under different environmental conditions the surface wetness can enhance or reduce O₃ deposition (Massman, 2004). For a boreal forest, a number of studies have revealed an enhancement of the O₃ uptake

under dew or high humidity conditions. For example, Lamaud et al. (2002) reported that dew on canopy surface significantly increased the O₃ uptake at night and in the morning over a pine stand. Altimir et al. (2006) also found that the condensed moisture on the surfaces enhanced the non-stomatal O₃ uptake in a Scots pine forest when ambient relative humidity (RH) was over 60 - 70%. Similarly to Altimir et al. (2006), Rannik et al. (2012) revealed a strong sensitivity of the nighttime O₃ uptake to RH. **The enhancement of O₃ uptake on wet leaf surface was also explained by previous studies which showed that both the micro structure of the leaf surface and the hydrophilic compounds existing on the leaf surface are able to facilitate the formation of the water films or clusters, although the foliage surface itself is hydrophobic (Altimir et al., 2006). As a result, the different dissolved compounds like organics in the solution formed on leaf surface could react with O₃ and thus enhance the O₃ uptake (Altimir et al., 2006).**

10 In addition, the boreal forest emits a large portion of BVOCs (Rinne et al., 2009) which are considered to play a significant role in non-stomatal removal of O₃ by oxidation in several studies (Kurpius and Goldstein, 2003; Goldstein et al., 2004; Wolfe et al., 2011). For example, Fares et al. (2010) found the correlation between the oxidation products of monoterpenes and O₃ non-stomatal flux at a ponderosa pine stand in California, US, indicating the gas-phase reactions of O₃ with BVOCs were mostly responsible for O₃ non-stomatal loss. In a model study, Wolfe et al. (2011) suggested that the non-stomatal O₃ uptake
15 at the same Californian site could be explained by considering the role of O₃ destruction with the presence of very reactive BVOCs. Consequently, further analysis of the role of non-stomatal removal of O₃ also strongly depends on the improvement of BVOCs measurement. However, the influence of this gas-phase chemical removal process may vary among different sites. A study by Rannik et al. (2012), who conducted a detailed analysis of a long-term O₃ deposition flux measurement at a boreal forest station in Hyytiälä, Finland, indicated that, at the currently known strength of BVOC emissions, the air chemistry of
20 BVOCs was not likely an important O₃ sink term at this site.

~~These removal processes altogether determine the contribution of O₃ uptake on forest ground surface and understory vegetation, the vertical distribution of O₃ concentration as well as the non-stomatal uptake contribution, which are considered as three crucial challenges to understand the relationship between the eddy-covariance measurements and O₃ uptake (Launiainen et al., 2013).~~ **Therefore** In recent two decades, several numerical models have been developed to study and simulate O₃ dry deposition processes under different climatic and environmental conditions ~~, which are generally based on the surface deposition model described by Wesely (1989). Among these models, the so-called "big-leaf" approach method is widely used and usually~~
25 **.** Many of them have implemented the big-leaf framework following the Wesely (1989) approach which can be coupled to regional or global models to estimate the O₃ deposition flux in large scales (e.g. Zhang et al., 2002)(e.g., Hardacre et al., 2015). However, the "big-leaf" approach does not consider explicitly the role of in-canopy interactions between biogenic emissions,
30 chemistry, turbulence and deposition. Therefore, more detailed multi-layer models including the role of these in-canopy interactions have been developed and applied to analyse in-canopy deposition-related mechanisms (e.g., Ganzeveld et al., 2002b; Rannik et al., 2012; Altimir et al., 2006; Launiainen et al., 2013). These multi-layer canopy exchange models have also been coupled to large scale models, e.g., a global chemistry-climate model system (Ganzeveld et al., 2002a), or have been implemented in column models with detailed vertically separated layers (e.g., Wolfe and Thornton, 2011). **Recent models have been**

~~developed more and more based on the physical, chemical and biological processes under actual environmental conditions, which reduce the dependency of empirical parameters (Wesely and Hicks, 2000).~~

In this study a multi-layer ~~process-based~~ O₃ dry deposition model was implemented into the 1-dimension (1D) chemical transport model SOSAA (a model to Simulate the concentrations of Organic vapours, Sulphuric Acid and Aerosols). This deposition model was based on the dry deposition representation originally described in Ganzeveld and Lelieveld (1995) and Ganzeveld et al. (1998) and implemented in the Multi-Layer Canopy CHEmistry Exchange Model (MLC-CHEM, ~~manuscript in preparation~~ Ganzeveld et al. (2002b)). This canopy exchange system in MLC-CHEM was already applied in a single column model on the analysis of site-scale exchange processes (Ganzeveld et al., 2002b; Seok et al., 2013), as well as in a global chemistry-climate model system on the analysis of atmosphere-biosphere exchange processes (Ganzeveld et al., 2002a, 2010).

Furthermore, the long-term continuous measurements and extensive campaigns at SMEAR II have provided a vast amount of data with complementary information on micrometeorology as well as O₃ fluxes and concentrations, which are highly appropriate for validating the new model and ~~also shining a light on those three challenges with the model~~ **investigating more detailed processes**. We selected a featured month August 2010 for such an extensive evaluation of the model because this month was characterised by exceptional hot and dry conditions in the first two weeks, which possibly represented a future climate at this site (Williams et al., 2011), then followed by two cooler weeks. This study is a starting point of investigating gas dry deposition processes ~~in~~ **by using** SOSAA. We aim to evaluate not only quantitatively O₃ fluxes and concentration profiles but also the role of individual deposition processes at this site. This is a prerequisite for a further analysis of BVOCs deposition and chemistry in the follow-up research.

In the following section, a detailed description of the measurement and model will be shown. ~~The comparison and analysis of observed and simulated meteorological quantities, O₃ fluxes, O₃ concentration profiles, chemical removal process and corresponding discussions are described in section 3, followed by a summary in section 4.~~ **The comparisons between simulated and observed meteorological quantities, O₃ fluxes above the canopy and O₃ concentration profiles are described in section 3, as well as the discussion about O₃ flux profiles and the impact of air chemistry. Finally, a summary is given in section 4.**

2 Methods

2.1 Site

All the measurement data used in this study were from SMEAR II (the Station to Measure Ecosystem-Atmosphere Relation II) located in Hyytiälä, Finland (61°51'N, 24°17'E, 181 m above the sea level) (Hari and Kulmala, 2005). The boreal coniferous forest is relatively homogeneous around the station in all the directions within 200 m, 75% covered by Scots pine (*Pinus sylvestris*) and the rest covered by Norway Spruces (*Picea abies*) and deciduous trees (Bäck et al., 2012). The understory vegetation mainly consists of lingonberry (*Vaccinium vitis-idaea*) and blueberry (*Vaccinium myrtillus*) with a mean height of 0.2 - 0.3 m. The forest floor is covered by dense mosses, mostly *Dicranum polysetum*, *Hylocomium splendens* and *Pleurozium schreberi*. Underneath is a 5 cm layer of humus in soil (Kolari et al., 2006; Kulmala et al., 2008). In 2010, the tree height reaches around 18 m. The all-sided leaf area index (LAI) is about 7.5 m² m⁻², including ~ 6.0 m² m⁻² overstory vegetation,

$\sim 0.5 \text{ m}^2 \text{ m}^{-2}$ understory vegetation and $\sim 1 \text{ m}^2 \text{ m}^{-2}$ moss layer (Launiainen et al., 2013). The vertical profiles of LAI and leaf area density (LAD) are shown in Fig. 1.

2.2 Measurements

The measurement data at SMEAR II are currently publicly available in the data server maintained by AVAA open data publishing platform (<http://avaa.tdata.fi/web/smart/smear>), which was originally introduced in Junninen et al. (2009). A part of observed quantities used in this study are available at 4.2 m, 8.4 m, 16.8 m, 33.6 m, 50.4 m and 67.2 m (above the ground level, ~~the same below~~, including air temperature (measured by Pt100 sensor), air water content (Li-Cor LI-840 infrared light absorption analyser) and O_3 concentration (TEI 49C ultraviolet light absorption analyser). Other observed quantities include the photosynthetically active radiation (PAR, 400–700 nm) (Li-Cor Li-190SZ quantum sensor) measured at 18 m, PAR (array of 4 Li-Cor Li-190SZ sensors) measured at 0.6 m, net radiation (Reeman MB-1 net radiometer) at 67 m, O_3 flux (Gill Solent HS 1199 sonic anemometer & Unisearch Associates LOZ-3 gas analyzer) at 23 m, friction velocity (Gill Solent 1012R anemometer/themometer) at 23 m, sensible and latent heat fluxes (H and LE) (Gill Solent 1012R and Li-Cor LI-6262 gas analyzer) at 23 m, and soil heat flux (Hukseflux HFP01 heat flux sensors).

In this study the measured O_3 fluxes were calculated over 30 min averaging period using the EddyUH software (Mammarella et al., 2016) and according to standard methodology (for more details see Rannik et al., 2012). Other variables were also half-hour averaged to fit the model time step for both input and output. The air temperature (T), RH and O_3 concentration were linearly interpolated using the observations collected at a height of 16.8 m and 33.6 m to arrive at the estimated parameter values at 23 m to allow a direct comparison of the model results with the measurements or being used as input for the model. ~~In addition, some of the observed parameters were also used to constrain the model simulations (see next section). The missing~~
observed data points of T , RH and O_3 were gap-filled with the method described in Gierens et al. (2014).

The measured O_3 fluxes were filtered based on the fact that previous studies showed that the measured fluxes had large errors under very low turbulence (Rannik et al., 2006). The threshold of such low turbulence condition was usually set according to the measured friction velocity on top of the canopy in the range of 0.1 m s^{-1} to 0.25 m s^{-1} (Altimir et al., 2006; Rannik et al., 2012; Launiainen et al., 2013). Here the observed O_3 fluxes were excluded when $u_* \leq 0.2 \text{ m s}^{-1}$ which was ~~consistent with~~
the study proposed by Rannik et al. (2012). Secondly, the O_3 flux measurements were filtered out when precipitation occurred within preceding 1 hour. Previous studies used a more strictly criteria for such a filter that the preceding 12 hours should keep dry to ensure dry canopy conditions (Altimir et al., 2006; Launiainen et al., 2013). However, in this study the fraction of wet canopy skin was taken into account and consequently we applied the filtering criteria of 1 hour. Overall, 5860% of O_3 flux data were available compared to 87% prior to filtering.

Here we should notice that the fluxes determined by the eddy-covariance (EC) technique were affected by the stochastic nature of turbulence, revealing as the random uncertainty of 30 min average fluxes. For the EC measurement the random uncertainty was typically in the order of ten to a few tens of percent. For the O_3 turbulent flux measurement at the same site Keronen et al. (2003) presented the random error statistics, defined as one standard deviation of the random uncertainty of turbulent flux, ranging from about 10 to 40%.

2.3 Classification of time period

Previous studies showed that in pine forest RH could enhance non-stomatal O₃ uptake (Lamaud et al., 2002; Altimir et al., 2006; Rannik et al., 2012), especially during nighttime (Rannik et al., 2012). Hence in order to further analyse the impact of RH, the data were separated into different groups according to daytime (D) and nighttime (N) as well as RH measured inside the canopy, representing the daytime with high humidity condition (DH), daytime with low humidity condition (DL), nighttime with high humidity condition (NH) and nighttime with low humidity condition (NL). The data points were considered as daytime when the sun elevation angle was larger than 10° and as nighttime when the sun elevation angle was smaller than 0°. The RH threshold value was set to 70% referring to previous studies (Altimir et al., 2006; Rannik et al., 2012), so a period is in high humidity condition when all the measured RH values inside the canopy are higher than 70%, similarly a period is in low humidity condition when all the measured RH values inside the canopy are lower than 70%. For O₃ flux, “ALL” was used to represent the time period with all available data after filtering described in section 2.2.

2.4 Model description

2.4.1 SOSAA

SOSAA is a 1D chemical transport model which couples different modules to simulate the emissions of BVOCs, chemical reactions of organic and inorganic compounds in the air, transportation of trace gases and aerosol particles, as well as the aerosol processes within and above the canopy in the planetary boundary layer. It was first introduced as SOSA by Boy et al. (2011) based on the 1D version of SCADIS (SCAlar DIStribution, Sogachev et al., 2002). After that an aerosol module based on UHMA (University of Helsinki Multicomponent Aerosol model, Korhonen et al., 2004) was implemented by Zhou et al. (2014) resulting in its name being changed to SOSAA. The current version of SOSAA includes five modules. The meteorology module is based on SCADIS. Emissions of BVOCs from the canopy are calculated by the Model of Emissions of Gases and Aerosols from Nature (MEGAN, Guenther et al., 2006). The Master Chemical Mechanism (MCM-v3.2) version 3.2 (MCMv3.2) (<http://mcm.leeds.ac.uk/MCM>) has been implemented to provide chemistry information. The nucleation, condensation, coagulation and deposition of aerosol particles are described by UHMA. In this study a gaseous compound dry deposition module has been implemented into SOSAA. SOSAA has already been applied and verified in several studies (e.g., Kurtén et al., 2011; Mogensen et al., 2011; Boy et al., 2013; Mogensen et al., 2015; Bäck et al., 2012; Smolander et al., 2014; Zhou et al., 2015).

SOSAA is partly constrained by SMEAR-II measurements and ERA-Interim reanalysis dataset provided by the European Centre for Medium-Range Weather Forecasts (ECMWF, Dee et al., 2011). The prognostic variables air temperature, horizontal wind speed and specific humidity near and within the canopy are nudged to local measurement data at every time step. In addition, the measurement data of soil heat flux, the incoming direct and diffuse radiations, along with the incoming long wave radiation are read in to modify the set-up of the system in order to simulate a realistic representation of the micrometeorology. It should be noted that the upward radiation at the canopy top, including the reflected and scattered short wave radiation as well as the emitted long wave radiation, is explicitly computed as a function of canopy structure parameters in SOSAA. The upward radiation is then used to calculate the net radiation on top of the canopy. The upper boundary conditions of air temperature,

horizontal wind speed and specific humidity are constrained by the reanalysis datasets. In SOSAA, the horizontal wind velocity (u and v), T , specific humidity (q_v), turbulent kinetic energy (TKE) and the specific dissipation of TKE (ω) are computed every time step (10 s) by prognostic equations. In order to represent the local to synoptic scale effects, u , v , T and q_v near and within the canopy are nudged to local measurement data at SMEAR II station with a nudging factor of 0.01. A TKE- ω parametrisation scheme is used to calculate the turbulent diffusion coefficient (K_t) (Sogachev, 2009),

$$K_t = C_\mu \frac{\text{TKE}}{\omega} \quad (1)$$

$$\omega = \frac{\varepsilon}{\text{TKE}} \quad (2)$$

where ε is the dissipation rate of TKE and C_μ (0.0436) is a closure constant. Hence the turbulent flux of a quantity X ($F_{t,X}$) can be computed as

$$F_{t,X} = -K_t \frac{\partial X}{\partial z} \quad (3)$$

where upward fluxes are positive and vice versa. Specifically, the sensible heat flux (H) and latent heat flux (LE) at each model layer are computed as

$$H = -C_{p,air} \rho_{air} K_h \left(\frac{\partial T}{\partial z} + \gamma_d \right) \quad (4)$$

$$LE = -L_v K_h \frac{\partial q_v}{\partial z} \quad (5)$$

where $C_{p,air}$ ($1009.0 \text{ J kg}^{-1} \text{ K}^{-1}$) is the specific heat capacity at constant pressure. ρ_{air} (1.205 kg m^{-3}) is the air density which is a constant in the model. γ_d (0.0098 K m^{-1}) is the lapse rate of dry air. L_v ($2.256 \times 10^6 \text{ J kg}^{-1}$) is the latent heat of vaporisation for water. K_h is the turbulent eddy diffusivity for heat fluxes, which is derived from K_t according to the atmospheric stability.

The upper boundary values of u , v , T and q_v are constrained by the ERA-Interim reanalysis dataset provided by the European Centre for Medium-Range Weather Forecasts (ECMWF, Dee et al., 2011). Above the canopy, the incoming direct and diffuse global radiations measured at SMEAR II station, and the long wave radiation obtained from the ERA-Interim dataset are read in to improve the energy balance closure. Then the reflection, absorption, penetration and emission of three bands of radiation (long-wave, near-infrared and PAR) at each layer inside the canopy are explicitly computed according to the radiation scheme proposed by Sogachev et al. (2002). At the lower boundary, the measured soil heat flux at SMEAR II is used to further improve the representation of surface energy balance. All the input data are interpolated to match the model time for each time step. With the input data, the mass and energy exchange between atmosphere and plant cover (including the soil underneath) and the radiation attenuation inside the canopy are optimal to simulate the micrometeorological drivers of O_3 deposition at this site.

In current SOSAA, a modified version of MEGAN has been used to simulate the emissions of BVOCs from the trees. The emissions of some important BVOCs are included, e.g., monoterpenes (α -pinene, β -pinene, Δ^3 -carene, limonene, cineol and other minor monoterpenes (OMT)), sesquiterpenes (farnesene, β -caryophyllene and other minor sesquiterpenes (OSQ)), 2-methyl-3-buten-2-ol (MBO). The chemistry mechanism is from MCMv3.2 including needed inorganic reactions and the full

MCM oxidation paths for methane (CH₄), isoprene, MBO, α -pinene, β -pinene, limonene and β -caryophyllene. We have also included the first-order oxidation reactions with OH, O₃, NO₃ for cineole, Δ^3 -carene, OMT, farnesene and OSQ. The related chemical reactions of stabilised Criegee intermediates (sCIs) with updated reaction rates from Boy et al. (2013) are also taken into account in current simulations. For more details about emissions and chemistry we refer to Mogensen et al. (2015).

5 2.4.2 Multi-layer O₃ dry deposition model

A gas dry deposition model has been implemented into SOSAA to investigate the influence of the dry deposition processes on the atmosphere-biosphere gas exchange and in-canopy gas concentrations. In this study we focus on the O₃ dry deposition since it is the basis of calculating the uptake of other trace gases, including BVOCs (Wesely, 1989). In this multi-layer dry deposition model the O₃ deposition flux is calculated at each layer as

$$10 \quad F_i = -[O_3]_i \cdot V_{d,i} \quad (i = 1, \dots, N) \quad (6)$$

where F is the O₃ deposition flux (ppbv $\mu\text{g m}^{-2} \text{s}^{-1}$), $[O_3]$ is the O₃ concentration (ppbv $\mu\text{g m}^{-3}$), V_d is the deposition velocity layer-specific conductance (m s⁻¹). The subscript i represents layer index. Layer 1 is the bottom layer including the soil surface and the understory vegetation where the moss layer is considered as part of the soil surface for simplicity. The overstory layers 2 to N include only vegetation surface, where N is the layer index at the canopy top.

15 V_d is calculated for bottom layer (layer 1) and overstory layers (layers 2 to N) differently. In addition, the deposition onto dry and wet parts of the leaf surface is considered separately. In overstory layers, only the deposition onto leaves is taken into account, while in the bottom layer the additional pathway of deposition onto the soil surface exists. Thus

$$V_{d,i} = \frac{\text{LAI}_i}{r_{veg,i}} + \frac{\delta_{i1}}{r_{ac} + r_{bs} + r_{soil}}. \quad (7)$$

20 ~~where LAI_i is the all-sided leaf area index for each layer (m² m⁻²), r_{veg} is the leaf surface resistance (s m⁻¹, the unit is the same for the resistances shown below), r_{soil} (= 600 s m⁻¹) is the soil resistance. The default value 400 s m⁻¹ of r_{soil} applied in Ganzeveld and Lelieveld (1995) is representative for global scale studies, turning out to result in too large soil removal in the simulations of this study. Hence a larger resistance value (600 s m⁻¹) has been applied here. r_{ac} is the resistance representing the turbulent transport from the reference height of the understory vegetation to the soil surface. Since the gas transport is explicitly calculated in SOSAA and the bottom layer height is only 0.3 m, the turbulence resistance between vegetation and ground is expected not to be an important factor for soil deposition, and consequently we have set r_{ac} to a very small value (1 s m⁻¹).~~ The Kronecker delta δ_{i1} ($\delta_{i1} = 1$ when $i = 1$; $\delta_{i1} = 0$ when $i \neq 1$) is used introduced here to simplify the formula.

When O₃ deposits onto the leaf surface, it has to pass through the quasi-laminar sublayer above the leaf surface at first, then diffuses into the stomata and is finally destroyed inside the stomatal pores reflected by negligible mesophyllie resistance. Alternatively, O₃ can deposit onto the leaf cuticle if the leaf is dry, or it is absorbed by the wet skin on leaf surface. So the leaf surface resistance r_{veg} for each layer can be calculated r_{veg} is the leaf surface resistance which represents how O₃ finally deposits onto different parts of leaf surface (Fig. 1). It can be calculated at each layer for needle leaves as

$$30 \quad r_{veg} = r_b + \frac{1}{\alpha 1 / (r_{stm} + r_{mes}) + (1 - f_{wet}) / r_{cut} + f_{wet} / r_{ws}}. \quad (8)$$

here r_b is the quasi-laminar boundary layer resistance over the leaf surface, which depends on molecular diffusivity and horizontal wind speed. r_{stm} is the stomatal resistance which is calculated from the evapotranspiration rate in SOSAA, r_{mes} ($= 1 \text{ s m}^{-1}$) is the mesophylllic resistance, r_{cut} ($= 10^5 \text{ s m}^{-1}$) is the cuticular resistance and r_{ws} ($= 2000 \text{ s m}^{-1}$) represents the uptake on leaf wet skin. α is a correction factor reflecting the leaf shape. For needle leaves, the uptake on stomata, cuticles and wet skins occur on all sides of leaves, so α is set to 1.0. While for broad leaves, the stomatal uptake only happens on one side, so α is 0.5. O_3 can deposit on a side without stomata or a side with stomata, hence r_{veg} is computed in a different way as

$$r_{veg} = 2 \left/ \left(\frac{1}{r_{veg1}} + \frac{1}{r_{veg2}} \right) \right. \quad (9)$$

$$r_{veg1} = r_b + \frac{1}{(1 - f_{wet})/r_{cut} + f_{wet}/r_{ws}} \quad (10)$$

$$r_{veg2} = r_b + \frac{1}{1/(r_{stm} + r_{mes}) + (1 - f_{wet})/r_{cut} + f_{wet}/r_{ws}}. \quad (11)$$

Here r_b is the quasi-laminar boundary layer resistance over the leaf surface, which depends on molecular diffusivity and horizontal wind speed (Meyers, 1987), and r_{stm} is the stomatal resistance which is derived from the stomatal resistance for water vapour (r_{stm, H_2O}) by a factor of the molecular diffusivity ratio,

$$r_{stm} = \frac{D_{H_2O}}{D_{O_3}} r_{stm, H_2O}. \quad (12)$$

Here D_{H_2O} and D_{O_3} are the molecular diffusivities of water vapour and O_3 , respectively. r_{stm, H_2O} is computed by SCADIS module in SOSAA and also used to calculate latent heat flux and thus the energy balance (Sogachev et al., 2002). r_{mes} (0 s m^{-1}) is the mesophylllic resistance which can be ignored for O_3 . r_{cut} (10^5 s m^{-1}) is the cuticle resistance and r_{ws} (2000 s m^{-1}) represents the uptake on leaf wet skin. Their values are taken from Ganzeveld and Lelieveld (1995). Canopy wetness is represented by the fraction of wet skin f_{wet} which is determined by RH according to Lammell (1999): (Lammell, 1999; Wu et al., 2003),

$$f_{wet} = \begin{cases} 1 & 0.9 \leq \text{RH} \\ \frac{\text{RH} - 0.7}{0.2} & 0.7 \leq \text{RH} < 0.9 \\ 0 & \text{RH} < 0.7 \end{cases} . \quad (13)$$

The threshold 70% is suggested in by Altimir et al. (2006).

In the model the O_3 concentration is calculated for each layer by the continuity equation r_{ac} is the resistance representing the turbulent transport from the reference height of the understory vegetation to the soil surface. Since the gas transport is explicitly calculated in SOSAA and the bottom layer height is only $\sim 0.3 \text{ m}$, the turbulence resistance between vegetation and ground is expected not to be an important factor for soil deposition, and consequently we have set r_{ac} to zero. r_{bs} is the soil boundary layer resistance which is calculated as (Nemitz et al., 2000; Launiainen et al., 2013)

$$r_{bs} = \frac{\text{Sc} - \ln(\delta_0/z_*)}{\kappa u_* g}. \quad (14)$$

Here Sc (1.07) is the Schmidt number for O_3 . κ is the von Kármán constant (0.41). $\delta_0 = D_{O_3}/(\kappa u_* g)$ is the height above ground where the molecular diffusivity is equal to turbulent eddy diffusivity. z_* (0.1 m) is the height under which the logarithmic wind

profile is assumed. u_{*g} is the friction velocity near the ground. r_{soil} is the soil resistance, 400 s m^{-1} is used here according to Ganzeveld and Lelieveld (1995). A sensitivity analysis for r_{soil} will be shown in section 2.6. The diagram of the resistance analogy parametrisation method described above is shown in Fig. 1. All the symbols are also explained and listed in Table 4.

In the model the evolution of O_3 concentration is calculated for each layer by the prognostic equation

$$5 \quad \frac{\partial[\text{O}_3]}{\partial t} = \frac{\partial}{\partial z} \left(K_t \frac{\partial[\text{O}_3]}{\partial z} \right) - \frac{F}{\Delta z} V_d[\text{O}_3]A + Q_{chem} \quad (15)$$

where K_t is the turbulent eddy diffusivity for O_3 and the first term on the right-hand side represents the vertical mixing of O_3 . Δz is the layer height. LAI effect is already included in the calculation of deposition velocity (Eq. (7)), hence it is not explicitly multiplied in this equation. In addition, the O_3 turbulent flux (F_t) in the model can be obtained as where the first term on the right-hand side represents the vertical mixing of O_3 . The second term is the sink by dry deposition which is non-zero only inside the canopy. The last one is chemistry production and loss of O_3 for each model layer. V_d is the layer-specific conductance at height z which already includes the uptake by the leaves, including the leaf stomata and cuticle, as well as the uptake by the soil for the understory layer (Eq. 7). We have also distinguished the difference in uptake by dry and wet leaves. A is a unit scale factor which is set to $1 \text{ m}^2 \text{ m}^{-3}$ here. All the other chemical compounds are also computed following this prognostic equation. According to Eq. 3 the O_3 turbulent flux F_t in the model can be obtained as

$$15 \quad F_t = -K_t \frac{\partial[\text{O}_3]}{\partial z}. \quad (16)$$

with positive values representing downward flux.

The diagram of the resistance analogy parameterisation method described above is shown in Fig. 1. All the symbols are also explained and listed in Table 4.

2.5 Model setup

20 In this study the newly implemented O_3 dry deposition module ~~has been~~ was applied to simulate the time period from Aug 1st to Aug 31st 2010 (Julian day 213 to 243). The model column domain was set from 0 m at ground surface up to 3000 m with 51 layers logarithmically configured, including the whole planetary boundary layer and part of the free atmosphere on top of it. We also constrained the model with the site-specific vegetation cover properties as presented before in section 2.1. The overstory layers only included needle-leaf ~~ved~~ part of Scots pine trees above ~ 0.3 m. Below that there was the understory vegetation and

25 ground surface. Since the understory consisted of vegetation with leaves instead of needles, ~~we set $\alpha = 0.5$ the parametrisation method~~ for the understory vegetation ~~was considered the~~ same as that for broad-leaved species. In order to secure a more accurate representation of canopy wetness which was also ~~relevant to the calculation of the O_3 deposition velocity, RH values inside the canopy were constrained with the measured data~~ relevant to the calculation of the layer-specific conductance for O_3 , RH values inside the canopy were calculated from the measured absolute humidity and simulated air temperature.

30 In addition, to secure a realistic simulation of O_3 in a column model like SOSAA we also forced the model's O_3 concentration at 23 m ~~towards the observed O_3 concentration to account for the advection of air masses (Fig. 2b). The O_3 concentrations at other heights inside the canopy were calculated from Eq. (16) to resemble the observed value every time step, the O_3 con-~~

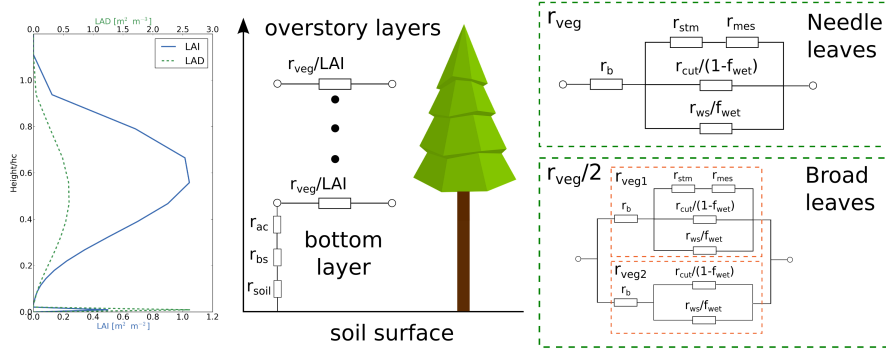


Figure 1. Vertical profiles of all-sided LAI (leaf area index) and LAD (leaf area density), as well as the diagram of resistance analogy method used in the O_3 dry deposition model. The overstory layers and the bottom layer are considered separately. The bottom layer includes the **broad-leaved** understory vegetation and soil surface. r_{ac} is the resistance representing the turbulent transport from the reference height of the understory vegetation to the soil surface. r_{bs} is the soil boundary layer resistance. r_{soil} is the soil resistance. r_b is the quasi-laminar boundary layer resistance above the leaf surface. r_{veg} represents the resistance to vegetation leaves, which is plotted on the right-hand side in details. Here r_b is the quasi-laminar boundary layer resistance above the leaf surface, For broad leaves, the resistance to the side with (r_{veg1}) or without (r_{veg2}) stomata is computed separately. r_{stm} is the stomatal resistance and r_{mes} is the mesophyll resistance. r_{cut} is the cuticular resistance, r_{ws} is the resistance to wet skin. f_{wet} is the wet skin fraction. α is a correction factor reflecting the leaf shape, which is 1.0 for needle-leaves and 0.5 for broad-leaves. All the variables are defined for each layer. Note that here LAI is the all-sided leaf area index for each layer. The symbols are also explained in the text and Table 4.

Table 1. Table of sensitivity cases. The case names and their short description texts are shown.

name	description
BASE	the same as described in section 2.4
RSOIL200	$r_{soil} = 200 \text{ s m}^{-1}$
RSOIL600	$r_{soil} = 600 \text{ s m}^{-1}$
RSOIL800	$r_{soil} = 800 \text{ s m}^{-1}$
FREEO3	O_3 concentration at 23 m was also computed instead of using observed data

centration at other levels were then calculated by Eq. 15. In this way, we implicitly added the role of advection in determining the O_3 concentration above the canopy. The gap-filled observed values which were used for the forcing are shown in Fig. 2b.

Several sensitivity cases have been conducted in this study (Table 1). In the case BASE all the parameters and methods were kept the same as described in section 2.4. In cases RSOIL200, RSOIL600 and RSOIL800 r_{soil} was altered to 200 s m^{-1} , 600 s m^{-1} and 800 s m^{-1} , respectively. In the case FREEO3, the O_3 concentration at 23 m was computed from Eq. (15) instead of being set to the measurement data.

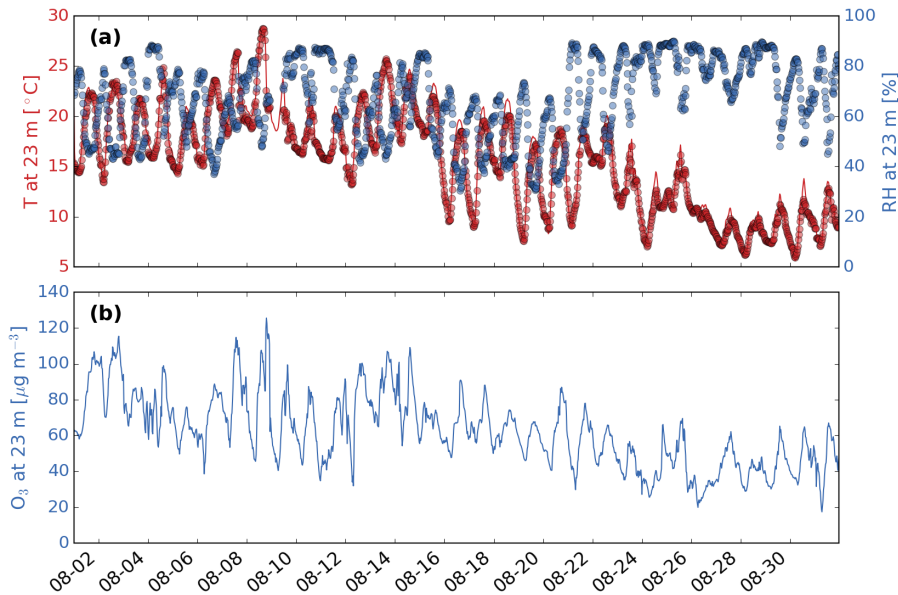


Figure 2. (a) Modelled (solid line) and measured (dots) time series of air temperature (**T**, red) and the measured ambient relative humidity (**RH**, blue) at **canopy top 23 m above the ground**. (b) **Gap-filled** Measured O₃ concentration (blue) at **canopy top 23 m above the ground**. The time period is August, 2010.

2.6 Sensitivity analysis of r_{soil}

r_{soil} varied in different studies, ranging from 10 to 180 s m⁻¹ for dry soil and 180 to 1100 s m⁻¹ for wet soil (Massman, 2004). In this study the dry deposition module was developed on the basis of the model from Ganzeveld and Lelieveld (1995) in which r_{soil} was 400 s m⁻¹. In order to assess the uncertainties involved in estimating r_{soil} , different values of r_{soil} ranging

5 from 200 to 800 s m⁻¹ were tested in this study (Table 2). As can be expected, the modelled O₃ fluxes decreases as r_{soil} increases. The BASE case shows the best performance in general, although it overestimates ~ 16% nighttime O₃ fluxes. Since the RSOIL200 case overestimates O₃ fluxes by ~ 17% in average for the whole month, ~ 12% at daytime and ~ 35% at nighttime, the RSOIL200 sensitivity case indicates that using this lower estimate, a value that might be more appropriate for high organic (and dry) soils, seems not to represent properly the role of soil removal at this site. On the other hand, taking

10 higher resistance values, e.g., one of 600 or 800 s m⁻¹ seems to result in a better simulation of the role of the soil uptake at nighttime. However, considering the overall performance and better estimation of daytime O₃ fluxes, we used 400 s m⁻¹ as the soil resistance in this study.

Table 2. The average (MEAN) and standard deviation (STD) of modelled and measured O_3 fluxes ($\mu\text{g m}^{-2} \text{s}^{-1}$) above the canopy during different time periods (ALL for the whole month, D for daytime, N for nighttime) for different cases (OBS for measurement, BASE for basic settings used in this study, RSOIL200 uses the same settings as in BASE except $r_{soil} = 200 \text{ s m}^{-1}$, similarly, RSOIL600 with $r_{soil} = 600 \text{ s m}^{-1}$ and RSOIL800 with $r_{soil} = 800 \text{ s m}^{-1}$) are shown. The relative error (RE) of modelled O_3 flux compared to the observation $(F_{t,mod} - F_{t,obs})/F_{t,obs}$ is also listed within the parentheses.

CASES	ALL		D		N	
	MEAN±STD	RE	MEAN±STD	RE	MEAN±STD	RE
OBS	0.246 ± 0.175		0.334 ± 0.165		0.103 ± 0.073	
RSOIL200	0.286 ± 0.173	+16.4%	0.375 ± 0.162	+12.1%	0.140 ± 0.067	+35.0%
BASE	0.250 ± 0.153	+1.77%	0.329 ± 0.143	-1.74%	0.120 ± 0.059	+16.2%
RSOIL600	0.231 ± 0.144	-6.00%	0.305 ± 0.134	-8.85%	0.109 ± 0.057	+5.16%
RSOIL800	0.219 ± 0.139	-10.8%	0.290 ± 0.129	-13.2%	0.101 ± 0.055	-2.17%

3 Results and discussion

3.1 Micrometeorology

The simulated month was warm and dry with little precipitation. Moreover, the temperature decreased dramatically in the middle of the month. In the first half of month (Aug 1st to Aug 15th) the average temperature at 23 m was 19.0 °C, while it dropped to 12.1 °C in the second half of month (Aug 16th to Aug 31st). ~~The time series of temperature especially this transition were well predicted by the model~~ (Fig. 2a). Analysis of the full temperature record indicated that this transition in the weather conditions at the site was well simulated by the model. RH varied inversely with air temperature. Its average value increased only slightly from 66.0% in the first half of the month to 69.3% in the second half. However, a dramatic increase of daily mean RH values from 49.3% to 73.5% occurred between Aug 20th and Aug 21st (Fig. 2a). The combination of the dry weather and the large variation of temperature provided a good sample for verifying the O_3 dry deposition module. ~~It was also interesting to study this featured time period with hot and dry climate which probably represented a future trend at this boreal forest site (Williams et al., 2011).~~

Figure 3 showed the comparison results between simulated and measured horizontal wind speed and friction velocity (u_*) which both were essential for estimating the turbulent transport above and within the canopy as well as for the calculation of the quasi-laminar boundary layer resistance of leaves (r_b) at each canopy layer and the soil boundary layer resistance (r_{bs}). Figure 3a showed the good agreement between modelled and measured monthly-mean horizontal wind speed profiles during both daytime and nighttime. The wind speed decreased quickly inside the canopy due to canopy drag, then changed little below $0.5 h_c$ until near the surface where wind speed varied logarithmically to zero on the surface. ~~The simulated turbulent mixing above and within the canopy was evaluated by comparisons of the modelled and measured friction velocity (Fig. 3b, 3c and 3d).~~ The model reproduced the diurnal cycle of u_* but overestimated the nighttime values by ~ 0.05

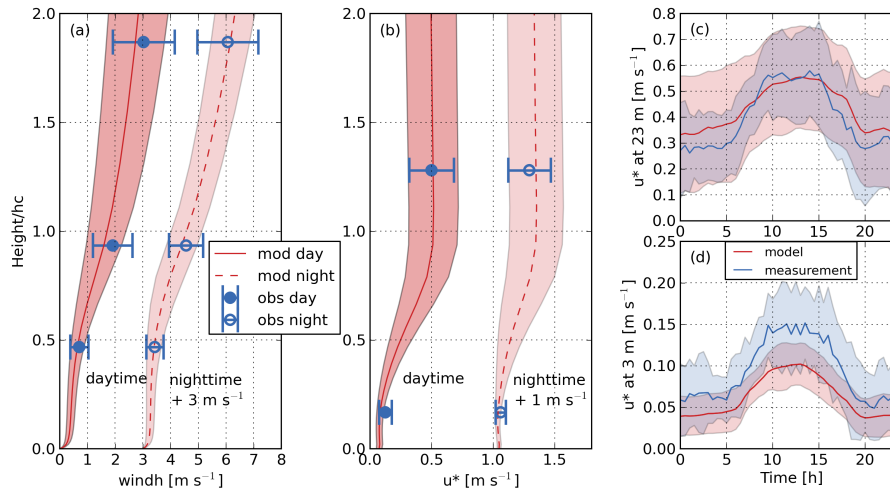


Figure 3. Modelled (red solid line for daytime, red dashed line for nighttime) and measured (blue solid circle for daytime, blue empty circle for nighttime) profiles of horizontal wind speed (windh) (a) and friction velocity (u_*) (b). Nighttime values are added/shifted by 3 and 1 m s^{-1} for windh and u_* for clarity of presentation, respectively. The ranges of ± 1 standard deviation of modelled and measured data are marked as shades and error bars. The height is normalized by canopy height h_c . The monthly-mean diurnal cycles of modelled (red) and measured (blue) friction velocity at 23 m and 3 m are shown in (c) and (d). The ranges of ± 1 standard deviation are marked as shades in the same colours.

m s^{-1} in average above the canopy top (Fig. 3c). Below the canopy crown at ~ 3 m, u_* was underestimated by ~ 0.02 m s^{-1} at nighttime and ~ 0.05 m s^{-1} at daytime (Fig. 3d). The discrepancy was likely due to the limitation of representing the real heterogeneous dynamics by a 1D model with homogeneous canopy configuration.

3.2 PAR above and below the canopy crown

- 5 Photosynthetically active radiation (PAR) plays an important role in stomatal exchange which determines to a large extent the daytime vegetation uptake. The PAR on top of the canopy was calculated directly from the input incoming short wave radiation with a daytime maximum of about $250\text{--}300$ W m^{-2} during the simulation month. Inside the canopy, PAR was calculated by considering the absorption, reflection and scattering effects of canopy leaves (Sogachev et al., 2002), which is predicted by the model well except slightly overestimation during daytime on several days. The PAR above the canopy is calculated directly from the measured incoming short wave radiation serving as input to the model, and shows a daytime maximum of about $250\text{--}300$ W m^{-2} during the simulation month. The PAR inside the canopy is calculated by considering the absorption, reflection and scattering effects of canopy leaves in the model (Sogachev et al., 2002). The comparison between modelled and observed PAR at ~ 0.6 m below the canopy crown was shown in Fig. 4. The monthly-mean diurnal cycle of attenuated PAR below the canopy crown in the model was consistent with the observation except two missing peaks at daytime (Fig. 4b). These two peaks in the measurement were the consequence of direct exposure of PAR sensors to incoming solar radiation. Such
- 15

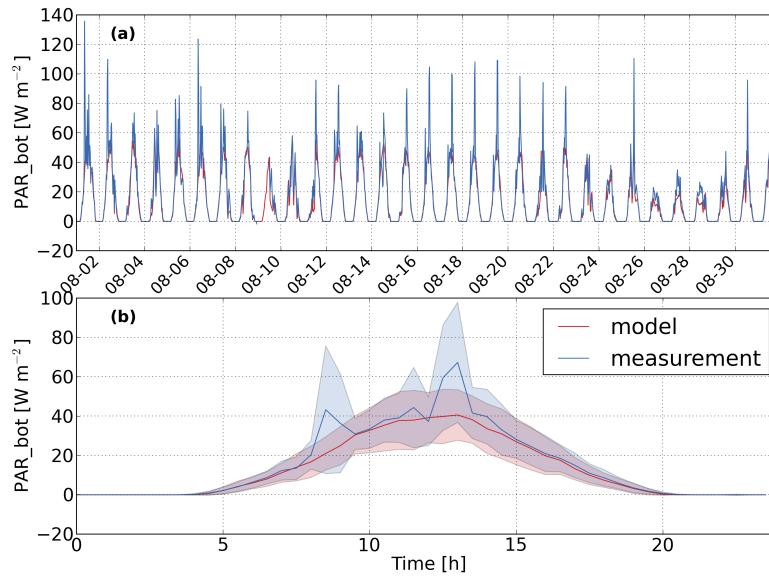


Figure 4. (a) Time series of PAR at 0.6 m from model (red) and measurement (blue) in August, 2010. (b) The monthly averaged diurnal cycle of time series in (a) for model (red) and measurement (blue). The range of ± 1 standard deviation is marked by the shade with the same colour.

situation always occurred when point-wise measurements were compared with a model assuming a homogeneous forest canopy.

3.3 Energy balance at canopy top

The monthly-mean diurnal cycles of sensible heat flux, latent heat flux, net radiation and soil heat flux, were shown in Fig. 5 in order to verify the simulated energy balance above the canopy in this study. The upward energy flux or the loss of surface energy was represented by positive values. During daytime, the soil and canopy lost energy by heat fluxes and gained energy mainly from net incoming solar radiation. At night, the surface lost energy by net upward long wave radiation with an average rate of $\sim 33 \text{ W m}^{-2}$, which was partly compensated by $\sim 20 \text{ W m}^{-2}$ downward energy from transport of warmer air.

During the simulation period the modelled diurnal cycles of energy fluxes agreed well with the observation, although, for example, the latent heat flux was slightly underestimated by $\sim 30 \text{ W m}^{-2}$ during daytime. In the afternoon from 14:00 to 20:00 the sensible heat flux was underestimated by $\sim 20 \text{ W m}^{-2}$. This could be explained by the underestimation in net radiation. However, the modelled values were generally within the one standard deviation range of the observations. The agreement between modelled and measured latent heat flux also indicated that the stomatal exchange, which controlled

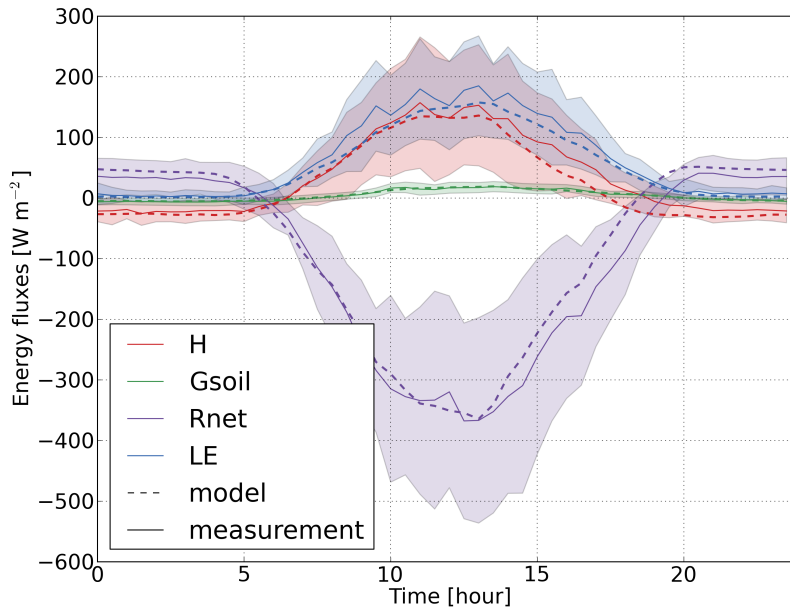


Figure 5. The monthly averaged diurnal cycle of different energy flux terms at [canopy top](#) (23 m above the ground) for model (dashed lines) and measurement (solid lines), including sensible heat flux (H, red line), soil heat flux (Gsoil, green line), upward net radiation (Rnet, purple line, note the observed Rnet is at 67 m), latent heat flux (LE, blue line). The range of ± 1 standard deviation for measurement data is plotted for every term by the shade with the same colour.

the latent heat flux and [was](#) directly related to the stomatal resistance of O_3 and many other gaseous compounds, [was](#) realistically simulated as a function of the meteorological drivers.

3.4 O_3 fluxes [at the canopy top](#)

The modelled time series of O_3 turbulent flux and its diurnal cycle [were](#) compared with the measurement data [at](#) the canopy [top](#) (Fig. 6). In general, the modelled flux showed a good agreement with the observations especially in the second half of month (Fig. 6a). Large discrepancies mostly occur in the first half of month which [was](#) warm and dry. On the first 3 days of the month, the O_3 turbulent flux [was](#) overestimated by the model. At noon on some days (e.g., Aug 9th, 12th, 13th, 14th, 27th, 30th), the model [was](#) not able to predict the observed high peaks of O_3 turbulent fluxes. [However](#) [In an average diurnal cycle of \$O_3\$ turbulent flux, the model does not capture the rapid increase of downward \$O_3\$ turbulent flux in the morning, but it follows the measurement well after 10:00. In general](#) the agreement between the simulated and measured monthly-mean diurnal cycles of O_3 turbulent fluxes [was](#) promising.

[Figure 7 showed the correlation between the simulated and measured \$O_3\$ turbulent fluxes at the canopy top for different humidity conditions at daytime and nighttime, separately. Previous studies showed that in pine forest RH could enhance](#)

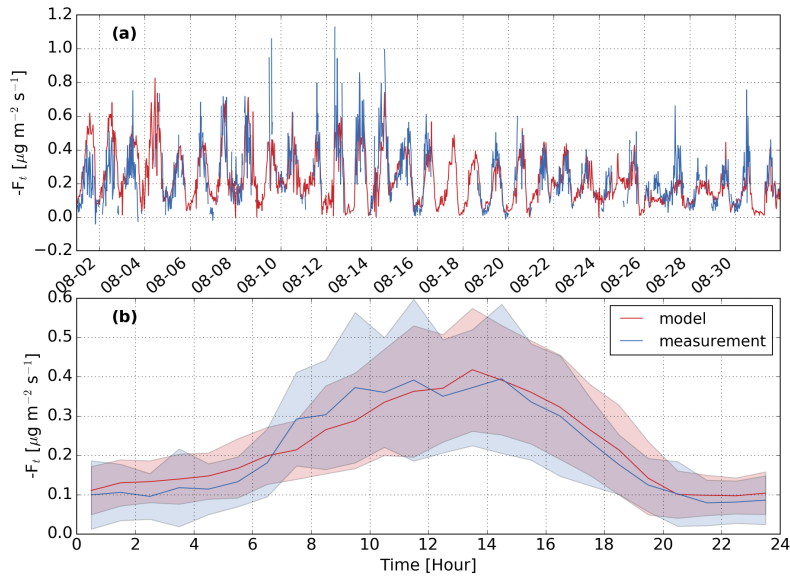


Figure 6. (a) Time series of the simulated (red) and measured (blue) O_3 turbulent fluxes ~~at above~~ the canopy ~~top~~ in August, 2010. (b) The monthly averaged diurnal cycles of time series ~~presented~~ in (a) for the model (red) and measurement (blue). The ranges of ± 1 standard deviation are marked by the shades with the same colours. **Positive values represent downward fluxes.**

~~both stomatal and non-stomatal O_3 uptake (Lamaud et al., 2002; Altimir et al., 2006; Rannik et al., 2012) especially during nighttime (Rannik et al., 2012). Hence in order to further analyse the impacts of RH, the data were separated into different groups according to daytime and nighttime as well as RH measured at 23 m, representing the daytime with high humidity condition (DH), daytime with low humidity condition (DL), nighttime with high humidity condition (NH) and nighttime with~~
 5 ~~low humidity condition (NL). The data points were considered as daytime when the sun elevation angle was larger than 10° and as nighttime when the sun elevation angle was smaller than 0° . The RH threshold value was set to 70% referring to previous studies (Altimir et al., 2006; Rannik et al., 2012).~~

Figure 7 shows the correlation between the simulated and measured O_3 turbulent fluxes above the canopy for different ~~humidity conditions at daytime and nighttime separately.~~ The overall R^2 between the modelled and measured O_3 turbulent
 10 ~~fluxes for the whole dataset was~~ 0.530.47. Among the four individual datasets under different conditions, the best prediction by the model ~~occurs~~ for the NH data points with R^2 of 0.360.37, followed by the ~~condition DH with R^2 of 0.30, both of them were under high humidity conditions. While under low humidity conditions, the correlation with the measurement data was much lower than that for the high humidity conditions. The R^2 of the condition NL was the smallest (0.10) (Fig. 7 and Table ??), results reflecting the daytime high humidity conditions ($R^2=0.19$).~~ Note that these conditions with highest correlations are
 15 ~~also the conditions with high relative humidity, especially at nighttime. All the correlations are significant ($p < 0.001$) except the condition NL for which R^2 is only 0.02 (Fig. 7). This indicates~~ the difficulty of simulating the O_3 turbulent flux in weak

turbulent and low humidity conditions at nighttime. Rannik et al. (2009) revealed that the nighttime O₃ turbulent flux ~~were~~was affected by vertical advection of O₃. Therefore, when wet skin uptake ~~was~~is small for the condition NL, the vertical advection, ~~which is not considered in the current model~~, could play a more crucial role in O₃ turbulent flux than deposition. On the other hand, ~~the observed~~there are only 69 observed data points in the condition NL ~~were more dispersed compared to other conditions~~ which indicated ~~larger random errors induced in measurement~~which implies larger random uncertainty. However, when the surface ~~was~~is wetter, the simulated nocturnal O₃ turbulent fluxes correlated~~s~~ much better with the measurement. In addition, the measurement data showed~~s~~a larger range of variation (~~0.0–0.6 ppbv~~about $-1.2 - 0.0 \mu\text{g m}^{-2} \text{ s}^{-1}$) compared to the range in the modelled O₃ turbulent flux (~~0.0–0.4 ppbv~~about $-0.8 - 0.0 \mu\text{g m}^{-2} \text{ s}^{-1}$), which implied~~s~~ that the model ~~did~~does not capture the O₃ turbulent flux peaks or the measurement ~~was more scattered due to random errors~~s are more scattered due to random errors. Regarding the low R^2 values here, we should consider ~~that the fluxes determined by the eddy-covariance (EC) technique were affected by the stochastic nature of turbulence, revealing random errors of 30 min average fluxes. For the EC measurement the random uncertainty was typically in the order of ten to a few tens of percent. For the O₃ turbulent flux measurement at the same site Keronen et al. (2003) presented the random error statistics, defined as one standard deviation of the random uncertainty of turbulent flux, ranging from about 10 to 40%~~the uncertainty of measured fluxes. Such uncertainty contributed~~s~~ to the data scattering when comparing the modelled and measured fluxes, such as in Fig. 7, and reduced~~s~~ the correlation statistics.

In general, the parameterisation of wet skin fraction (Eq. (13)) and its impact on O₃ non-stomatal removal seemed~~s~~ to represent the O₃ deposition mechanisms inside the canopy well considering the good performance under high humidity conditions. Although the prediction of O₃ turbulent flux with weak turbulence at night under low humidity condition still had~~s~~ large uncertainties (Fig. 7), the simulated average nocturnal O₃ turbulent flux ~~at~~above the canopy ~~top~~ showed~~s~~ a good agreement with the observation (Fig. 6b).

3.5 O₃ concentration profile

In order to evaluate if the good agreement between the observed and simulated O₃ turbulent fluxes ~~at~~above the canopy ~~top~~ also implied~~s~~ a realistic representation of the O₃ concentration inside the canopy, we have conducted an evaluation of the simulated in-canopy O₃ concentration profile. The one-month averaged O₃ concentration profiles from model results and measurement~~were~~are shown in Fig. 8. The huge ~~error bars~~variation range resulted~~s~~ from the meteorological variations in this month, especially the dramatic transition in the middle of the month (Fig. 2). The average O₃ concentration of the whole month ~~was~~31.7 ppbv~~is~~ $60.4 \mu\text{g m}^{-3}$ at 23 m, then decreased~~s~~ gradually inside the canopy to ~~28.3 ppbv~~54.1 $\mu\text{g m}^{-3}$ at 4.2 m due to the in-canopy sinks, which ~~were~~are most likely dominated by deposition. Similar vertical gradients ~~were~~are also found for the four different conditions. At night, the turbulent mixing ~~was~~is smaller compared to daytime which inhibited~~s~~ the downward transport of air mass with larger concentration of O₃ into the canopy. Hence the O₃ removal by canopy and especially by soil surface resulted~~s~~ in larger gradient of O₃ inside the canopy during nighttime (Fig. 8).

The model results of O₃ concentration profiles showed~~d~~a good agreement with the observations~~s~~ except the slight overestimation for the DH condition below $\sim 8 \text{ m}$ ($0.45 h_c$) and the apparent underestimation for the NL condition throughout the

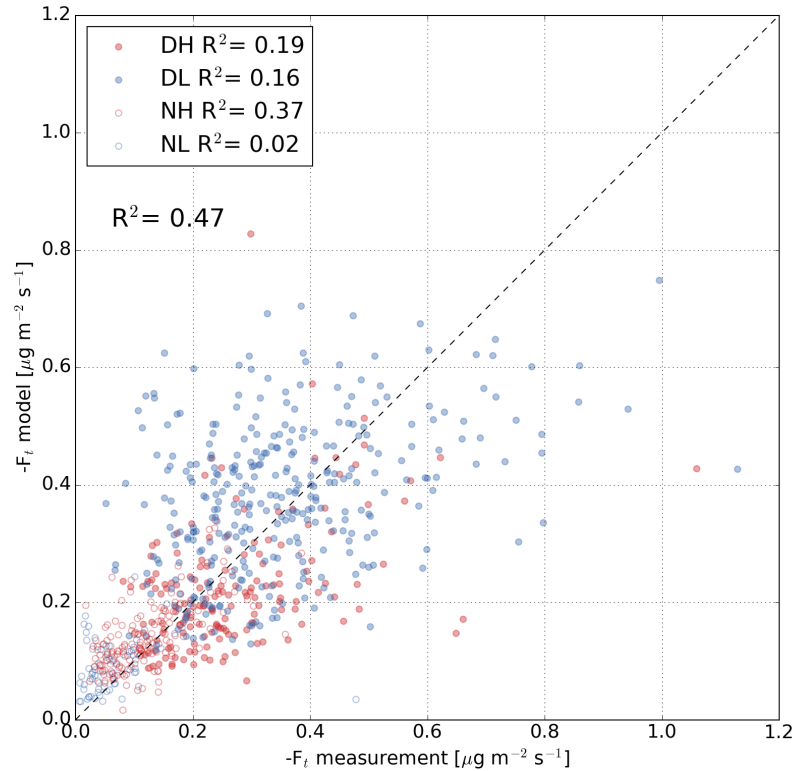


Figure 7. Scatter plots of modelled versus measured O_3 turbulent fluxes at above the canopy top. Four conditions of data points, including daytime points under high (labelled as DH, red solid circle) and low humidity conditions (labelled as DL, blue solid circle), nighttime points under high (labelled as NH, red empty circle) and low humidity conditions (labelled as NL, blue empty circle), are marked separately. The R^2 values are also labelled in the legend for four conditions. The data points are plotted separately for different groups (DH, DL, NH and NL) with their R^2 values shown in the legend. R^2 of the whole dataset is shown below the legend.

whole canopy. This was consistent with the model results of the O_3 turbulent fluxes, which showed 15.6% ~ 20% underestimation for the DH condition and 60.3% ~ 38% overestimation for the NL condition. In addition, the modelled vertical gradient of O_3 concentration during nighttime at drier conditions (NL) was much larger inside the canopy compared to the measured gradient, which implied that the soil deposition was largely overestimated when the soil and dry vegetation surface uptake dominated the overall removal inside the canopy. This also indicates that further investigation is needed for the more precise representation of ground surface deposition at different humidity conditions, including possibly the roles of uptake by the moss layer and soil humus layer.

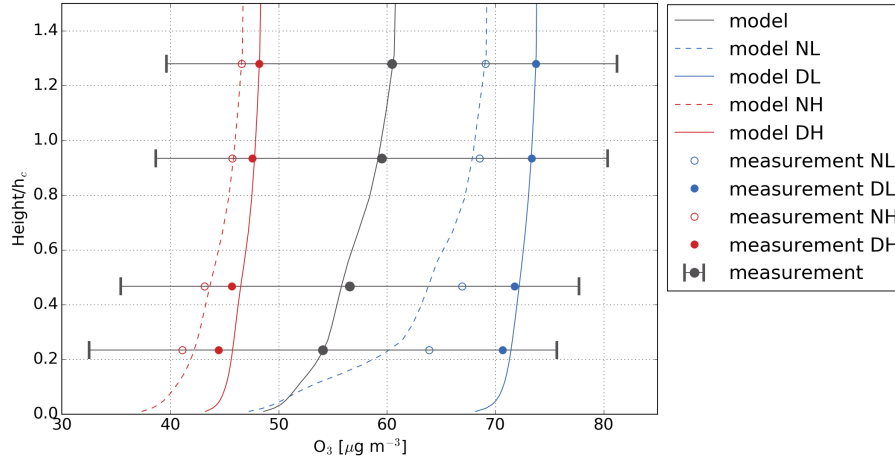


Figure 8. Measured average vertical profiles of O_3 concentration for the whole month (dark grey, the error horizontal bars are ± 1 standard deviations) and individual conditions (daytime under high humidity condition, labelled as DH with red filled circle; daytime under low humidity condition, labelled as DL with blue filled circle; nighttime under high humidity condition, labelled as NH with red empty circle; nighttime under low humidity condition, labelled as NL with blue empty circle). Modelled results are plotted as solid lines (daytime) and dashed lines (nighttime) with the same colour as measurement. The height is normalised by the canopy height h_c .

3.6 O_3 flux profile

The modelled vertical profiles of cumulative O_3 deposition flux ($\sum_{k=1}^i F_k$) normalised by the integrated O_3 deposition flux ($\sum_{k=1}^N F_k$) inside the canopy as well as the contributions of different deposition pathways for four different conditions were shown in Fig. 9. The normalised cumulative O_3 deposition flux at layer i can be obtained as

$$5 \quad F_{c,i} = \frac{\sum_{k=1}^i F_k}{\sum_{k=1}^N F_k} \quad (17)$$

where F_k is the O_3 deposition flux at layer k and N is the layer index just above the canopy. The profiles of F_c and the contributions of different deposition pathways for four different conditions are shown in Fig. 9. For the whole month, the O_3 uptake was dominated by soil deposition below $0.2 h_c$ (~ 3.6 m) with little only $\sim 8\%$ contribution from the understory vegetation via stomatal uptake. From $0.2 h_c$ to $0.8 h_c$ (~ 14.4 m) the cumulative uptake on leaf surfaces increased with height due to dense leaves in the plant crown area. Within this height interval, Above $0.8 h_c$ there only remains small portion of biomass ($\sim 7\%$) providing less than 2% O_3 uptake compared to the total O_3 deposition.

The soil uptake contributes to the total O_3 deposition flux at both daytime and nighttime (Figs. 9b and 9c) with a percentage of $\sim 32\%$ and $\sim 54\%$, respectively. At daytime, $\sim 63\%$ of the O_3 deposition flux is due to stomatal uptake. While at nighttime, when RH is larger than 70% at most of the time, the cumulative wet skin uptake contributes $\sim 41\%$ to the total O_3 deposition. At nighttime under high humidity conditions, the wet skin uptake even contributes $\sim 51\%$ to the total O_3 deposition fluxes (Table 3). This indicates that wet skin uptake relevant to RH plays a crucial role at night which is consistent with the results

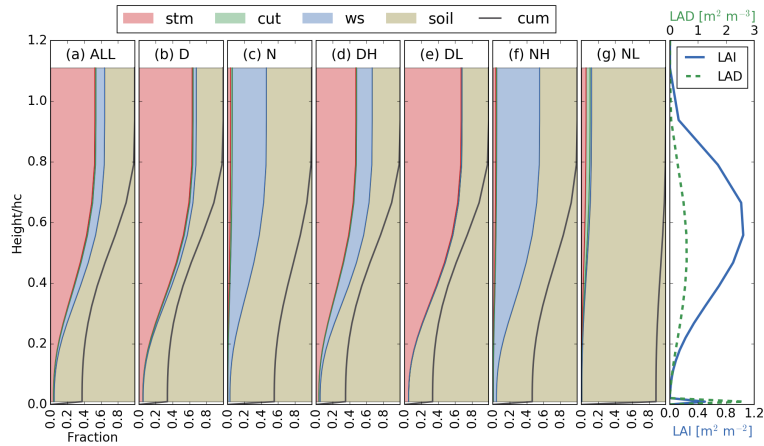


Figure 9. Simulated vertical profiles of cumulative O_3 deposition flux normalised by the integrated O_3 deposition flux **at** above the canopy **top** (cum, solid black line) for four conditions DH (a), DL (b), NH (c) and NL (d). D and N represent daytime and nighttime, H and L represent high and low humidity, respectively. Shaded areas are the cumulative contribution fractions for different deposition pathways, including stomatal uptake (stm, red), cuticular uptake (cut, green), wet skin uptake (ws, blue) and soil uptake (soil, pale brown). The all-sided LAI profile for each layer and LAD is plotted again here (e). The height is normalised by the canopy height h_c .

in Rannik et al. (2012). As a result, the simulated averaged non-stomatal contribution to the integrated O_3 deposition flux above the canopy is $\sim 37\%$ during daytime and $\sim 96\%$ during nighttime (Table 3). It should be noted that the stomata are not completely closed at night (Caird et al., 2007) and the minimum stomatal conductance at nighttime is about 5% of its maximum value at daytime (Kolari et al., 2007) which is similar with the simulation result here ($3.7\%/63.0\% \approx 6\%$, Table 3).

- 5 Above $0.2 h_c$, the stomatal uptake (DL, Fig. 9b), wet skin uptake (NH, Fig. 9c) or both of them (DH, Fig. 9a; NL, Fig. 9d) started to play a significant role in the cumulative O_3 deposition fluxes. Finally, Hence at $0.8 h_c$ the cumulative contribution of soil deposition **was** less than 50% except in the NL condition when both the **cumulative** stomatal uptake and wet skin uptake **were** limited. In all **the four** conditions the dry cuticular uptake **was** minor with a maximum contribution of **3** about 5.0% for the NL condition. **It should be pointed out that during nighttime at low humidity conditions, the uptake onto wet skin could**
- 10 **still exist because the RH inside the canopy at night was usually larger than that at the canopy top. Therefore, although the RH at 23-m was lower than 70%, there could be still quite humid conditions prevailing inside the canopy. At nighttime under high humidity conditions, the wet skin uptake contributed nearly 50% to the total O_3 deposition fluxes (Table 3). This indicated the wet skin uptake relevant to RH played a crucial role at night which was consistent with the results in Rannik et al. (2012). Nearly all of the O_3 uptake occurred below $0.8 h_c$ (~ 14.4 m), above this height there only remained small portion of biomass**
- 15 **($\sim 7\%$) providing limited O_3 uptake compared to the total O_3 deposition.**

As a result, the simulated non-stomatal contribution to the integrated O_3 deposition flux at the canopy top varied from 33–56% during daytime to 85–92% during nighttime (Table 3). During daytime the sub-canopy layer (lower than 4.2 m according to Launiainen et al. (2013)) including soil surface, contributed about 40–38% to the integrated O_3 deposition, which

Table 3. The first four columns are the contribution fractions of different deposition pathways (stm as stomatal uptake, wet as wet skin uptake, cut as cuticular uptake, soil as soil surface uptake) in the integrated O_3 deposition flux inside the canopy in the model. The last column is the sub-canopy (below 4.2 m) O_3 turbulent flux ($F_{t,mod}(4.2m)$) compared to the O_3 turbulent flux ~~at~~above the canopy ~~top~~ ($F_{t,mod}$) in the model. Different conditions are listed along the row. D and N represent daytime and nighttime, H and L represent high and low humidity, respectively. ALL is for the whole dataset.

	stm	wet	cut	soil	$F_{t,mod}(4.2m)/F_{t,mod}$
D	63.0%	3.79%	1.12%	32.1%	38.0%
N	3.70%	40.5%	1.87%	53.9%	59.5%
DH	44.347.2%	22.018.5%	0.80.94%	32.933.4%	39.539.6%
DL	66.767.1%	-0.00.00%	1.21.17%	32.031.8%	37.837.6%
NH	-8.03.28%	48.651.0%	0.81.04%	42.644.7%	49.451.4%
NL	15.55.42%	18.21.78%	3.04.73%	63.488.1%	67.689.5%
ALL	47.852.5%	14.510.4%	1.21.25%	36.535.8%	42.541.7%

~~wasis~~ consistent with the results from Launiainen et al. (2013) in which the sub-canopy (lower than 4.2 m) contribution was 35–45% at daytime. At night the contribution increaseds to around 40% ~~to~~ 6560% due to the closed stomata in crown layers. This ~~wasis~~ much higher than that (25 – 30%) in Launiainen et al. (2013) (Table 3). The overestimation could result from the underestimation of the soil resistance, which ~~wasis~~ difficult to determine in such a complex ground ecosystem. However, among these four different conditions with the same constant soil uptake efficiency, only under the nocturnal dry conditions (NL) there ~~wasis~~ apparently an overestimation in O_3 uptake and consequently underestimation of the O_3 concentration inside the canopy (Fig. 8). Therefore, we expect that the poor performance for the NL condition ~~NL~~ also resulteds from the limitation of EC measurement technique under weak turbulence near the ground, and ~~ed~~ data amount under this condition (only 69 data points) which leads to larger ratio of random uncertainty and thus smaller R^2 .

Moreover, the assumption that the resistance r_{ac} between the understory vegetation and ground ~~wasis~~ not a limiting factor for soil deposition might not hold under certain conditions. On the other hand, Launiainen et al. (2013) studied one month earlier (July 1st to August 4th, 2010) than the time period (August 1st to August 31st, 2010) in this study, so the difference between these two studies could also be due to the meteorological and biological variations during the two summer months. However, the daytime contribution of the sub-canopy layer ~~wasis~~ consistent, so the difference between the two months could only play a minor effect.

3.7 ~~Chemical-removal-process~~Contribution of air chemistry

The role of chemical processes in explaining the O_3 removal inside the forest canopy have been discussed in previous studies (e.g., Altimir et al., 2006; Wolfe et al., 2011; Rannik et al., 2012; Launiainen et al., 2013). A study by Wolfe et al. (2011) found that the non-stomatal uptake over a Ponderosa pine stand in the US was associated with additional very reactive BVOCs

being present besides the identified ones. On the other hand, Rannik et al. (2012) suggested that the air chemistry provided only minor contribution at SMEAR II. ~~In this study we calculated the time scales of different removal processes to estimate the contribution of air chemistry. Although the time scale might not be a good criteria of chemical influence (Wolfe et al., 2011), it was still acceptable for a first qualitative estimate of the role of in-canopy chemistry on O₃ removal inside the forest canopy.~~ In order to estimate the contribution of chemical removal at SMEAR II, two different studies applied multi-layer models (Rannik et al., 2012; Launiainen et al., 2013) to simulate the O₃ fluxes and concentration inside the boreal forest canopy. However, both of them showed their limitations on estimating the chemical contribution. Rannik et al. (2012) only considered one chemical reaction of O₃ with β -caryophyllene. While in Launiainen et al. (2013), they simplified the chemical production and loss of O₃ with only two parameters to represent the first-order kinetic sink and photo-chemical production. In this study, we implemented a chemistry module with a detailed list of chemical reactions (see section 2.4.1), which was able to provide a more accurate estimation of chemical removal of O₃ inside the canopy.

~~The average value of measured O₃ flux ($F_{O_3,avg}$) in August, 2010 on top of the canopy was 0.17 ppbv m s⁻¹ at daytime and 0.05 ppbv m s⁻¹ at nighttime.~~ In order to get rid of the effect of synoptic-scale transport of O₃ and only focus on the local sinks and sources, we applied the simulation case FREEO3. In this simulation case we ignored the role of advection and only considered the role of local sources and sinks inside the canopy, i.e., dry deposition, chemical production and loss, and turbulent transport. Here the time period from Aug. 5th to 14th were selected from the simulation results to analyse the local chemical contribution, because the modelled O₃ concentration fitted to the measurement the best during this period out of the whole month for the case FREEO3, which indicated that the advection also did not have apparent effect on the local observed O₃ variation. The daily averaged (from Aug. 5th to 14th) production and loss of O₃ inside the canopy caused by dry deposition (F_{depo}) and chemistry (F_{chem}) are plotted in Fig. 10. The unit $\mu\text{g m}^2 \text{s}^{-1}$ means how much $\mu\text{g O}_3$ inside the canopy alters per unit square meter per second. So positive values correspond to O₃ production and negative values represent O₃ loss. Here the chemistry production is a net effect of O₃ loss reactions and photo-chemical production. F_{depo} (obviously negative) shows a maximum O₃ loss rate at about 14:00. While the chemistry produces O₃ from morning at \sim 06:00 to the afternoon at \sim 15:00, and destroys it throughout the other time of the day, especially at nighttime (Fig. 10). The ratio between F_{chem} and F_{depo} shows that chemical removal has its largest contribution of \sim 9% of the dry deposition sink in average at nighttime from 20:00 to 04:00. At daytime, our model simulation indicates that the O₃ production caused by chemistry can compensate up to \sim 4% of dry deposition loss in average. However, during the selected period, the chemical contribution and compensation can reach up to \sim 24% and \sim 20% at most. This indicates that in general chemistry has minor impact on O₃ alteration, but at some specific time the chemical production and removal of O₃ can still play a significant role.

As a comparison, we also calculated the time scales of different removal processes to estimate the contribution of air chemistry. The average value of measured O₃ flux ($F_{O_3,avg}$) in August, 2010 above the canopy was $0.33 \mu\text{g m}^{-2} \text{s}^{-1}$ at daytime and $0.10 \mu\text{g m}^{-2} \text{s}^{-1}$ at nighttime whereas the O₃ concentration ($[O_3]$) inside the canopy was about ~~32 ppbv~~ $61.6 \mu\text{g m}^{-3}$ during daytime and ~~26 ppbv~~ $50.5 \mu\text{g m}^{-3}$ at night on average. So the time scale of total O₃ flux (τ_{O_3}) could be obtained from

$$\tau_{O_3} = [O_3] h_c / F_{O_3,avg} \quad (18)$$

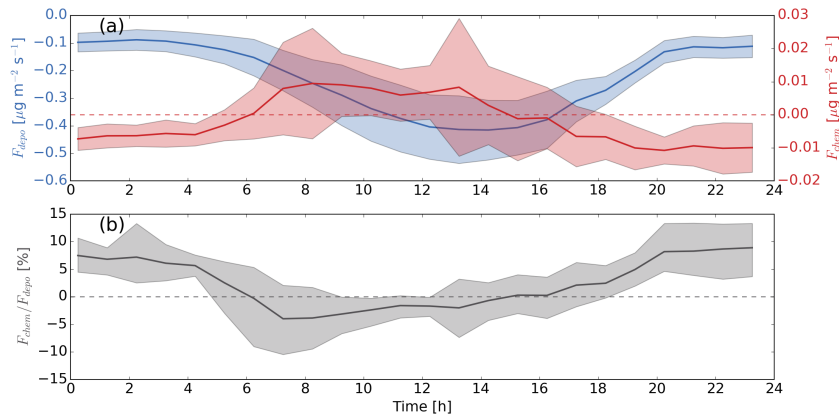


Figure 10. (a) The daily averaged (from Aug. 5th to 14th) production and loss caused by chemistry (F_{chem} , red) and dry deposition (F_{depo} , blue). (b) The ratio between F_{chem} and F_{depo} . Zero lines for F_{chem} and the ratio are plotted as dashed lines. Shaded areas show the range of ± 1 standard deviation.

which was 3384~3400 s (~ 1 h) for daytime and 9349~9100 s (~ 2.5 h) for nighttime. On the other hand, the total O₃ reactivity (y) at 18 m during a similar time period and at the same boreal forest station was calculated by Mogensen et al. (2015), which was $1.58 \times 10^{-5} \text{ s}^{-1}$ and $1.67 \times 10^{-5} \text{ s}^{-1}$ for noon and 2 a.m. at night. If the same values were assumed to be applicable also inside the canopy, the time scale of the O₃ removal by chemistry (τ_{c,O_3}) was

$$5 \quad \tau_{c,O_3} = y^{-1} \quad (19)$$

which was 63291~63300 s (~ 18 h) for daytime and 59880~59900 s (~ 17 h) for nighttime. These estimates showed that the chemical removal accounted for about 5% (3400/63300) and 15% (9100/59900) of the total O₃ removal within the canopy at daytime and nighttime, respectively. Thus during daytime the chemical removal affected only marginally the O₃ concentration within the canopy as compared to deposition and during the nighttime the effect was somewhat larger. It should be noted that this estimate was based on the current knowledge of air chemistry which could largely underestimate O₃ reactions with oxidised VOCs (Mogensen et al., 2015). Hence the chemical removal of O₃ might be larger than calculated here.

Turbulent transport within the canopy occurred at much shorter time scales than deposition and chemistry. For the same site Rannik et al. (2009, 2015) have estimated the time scale of turbulent transport within the canopy to be in the order of one minute for daytime and about ten minutes for nighttime conditions. This was typically shorter than the deposition time scale and much shorter than the time scale of chemical removal. In addition, the vertical flux was affected only if the chemistry modified the O₃ concentration differentially with height. Therefore the sinks or sources due to chemistry were likely to only introduce concentration change within the atmospheric column that is much higher than the forest layer.

Compared to the simulation results, the time scale analysis could not reflect the photochemical production of O₃ during daytime, hence the estimation of net chemical effects is not possible with this method. For nighttime, the time scale analy-

sis overestimates the average contribution of chemical removal by about 88% (15% compared to 8%, 8% is obtained from 9%/(100%+9%)). The comparison result could act as a proof of the statement in Wolfe et al. (2011), which argued that the time scale might not be a good criteria of chemical influence.

4 Summary

5 A detailed multi-layer O₃ dry deposition model has been implemented into SOSAA to investigate the O₃ uptake by canopy and soil surface at a boreal forest station SMEAR II. The presented detailed analysis of the O₃ deposition processes for this site was also motivated by the fact that it informed us about the representation of also quantified various removal processes, e.g., by the dry and wet cuticle, by stomatal uptake and by the soil surface, which were also involved in the removal of BVOCs and their oxidation products. In this model the fraction of wet skin on canopy leaves was parameterised according to RH values to analyse the potential role of canopy wetness on O₃ deposition for both high and low humidity conditions. Moreover, the multi-layer model also enabled the study of deposition processes inside the canopy and the partitioning of O₃ deposition fluxes between the canopy crown and sub-canopy. In this study, the model has been validated by comparing the modelled and measured O₃ turbulent flux at above the canopy top and its concentration profile inside the canopy.

Further investigation has been done through a more in-depth correlation analysis on O₃ turbulent fluxes for nighttime and daytime under high and low humidity conditions. The simulated O₃ turbulent fluxes at above the canopy top correlated reasonably well with the measurement for the whole month with R^2 of 0.530.47 ($p < 0.001$), which was also consistent with the plausible prediction of O₃ concentration profile inside the canopy. The good agreements significant correlation ($p < 0.001$) also applied to the daytime humid and dry as well as nighttime humid conditions (DH, DL and NH) with R^2 of 0.300.19, 0.210.16 and 0.360.37. However, the model was not able to predict high peaks with O₃ turbulent fluxes larger than 0.4 ppbv or 0.8 $\mu\text{g m}^{-2} \text{ s}^{-1}$. The model also did not capture well the measured O₃ removal for the nocturnal dry condition (NL), in which R^2 was only 0.100.02 and the O₃ concentration inside the canopy was largely underestimated (Figs. 7 and Table ??8). The possible reasons were expected to be the limitation of EC measurement technique under weak turbulence below the canopy crown at nighttime and the excessive ground deposition could be the limited data amount implying larger random uncertainty.

Nearly all of the O₃ uptake occurred below 0.8 h_c inside the canopy. During daytime, the contributions of both stomatal uptake (44.3~47%) and wet skin uptake (22.0~19%) and soil uptake (~33%) were significant in for the total O₃ uptake under high humidity conditions. While under low humidity conditions the stomatal (66.7~67%) and soil uptake (32.0%) contributed dominantly the overall canopy deposition. During nighttime, the stomatal uptake contribution (8.0~3%) was not zero, but was much smaller compared to the wet skin uptake (48.6~51%) under high humidity conditions. For the low humidity condition at night (NL), the contributions of stomatal uptake (15.5%) and wet skin uptake (18.2%) were similar and both of them were smaller than the soil deposition (63.4%). Therefore, the canopy wetness was considered to play a more crucial role at nighttime, especially under the high humidity condition. nearly all the deposition (~88%) was due to soil uptake. Since RH was larger than 70% at most of the time during night, the uptake by wet canopy could be a dominant factor for the nocturnal O₃ removal.

In addition, the simulated non-stomatal contributions to the integrated O₃ deposition fluxes were estimated as ~~55.7%, 33.3%, 92.0% and 84.5%~~ about 53%, 33%, 97% and 95% for conditions DH, DL, NH and NL, respectively (Table 3).

The modelled contribution of sub-canopy deposition during daytime (~~~ 40~~38%) was consistent with that (35 – 45%) in Launiainen et al. (2013), but it was much higher at nighttime (~~about 40 – 65 ~ 60%~~) compared to that in the same study (25 – 30%) (Table 3). This discrepancy at nighttime was most likely due to the overestimation of soil uptake. ~~This also indicated the difficulty of simulating and measuring O₃ deposition at night with weak turbulence (Rannik et al., 2009).~~

The contribution of O₃ removal by chemical reactions with currently identified BVOCs have also been ~~qualitatively estimated via the analysis of time scales. At daytime, a small fraction of about 5% of O₃ removal resulted from air chemistry compared to deposition. And at nighttime the fraction was about 16%.~~evaluated. In general the air chemistry played a minor role in O₃ uptake inside the canopy. In the simulated averaged diurnal cycle, the air chemistry produced O₃ during daytime from about 06:00 to 15:00, compensating up to 4% of dry deposition sinks. While at nighttime, the chemical loss enhanced O₃ removal by ~ 9% of that by dry deposition. A qualitative estimation of chemical contribution with time scale analysis was also conducted as a comparison. However, this method overestimated the air chemical removal by about 88% for nighttime and it was not able to reflect the O₃ production at daytime.

This study is the first step to establish a detailed gas dry deposition model in SOSAA. Further ~~implementa~~analysis of dry deposition will be done for other chemical compounds, especially for BVOCs. This will improve not only the ability ~~of to~~ simulate air chemistry and aerosol processes but also our understanding of the mechanisms involved in the removal processes at boreal forest. In addition, it is also of scientific interest~~ing~~ to investigate how future climate change might ultimately affect the removal processes of compounds like O₃ and BVOCs for boreal forests.

20 Appendix A: Table of symbols

Table 4: Table of symbols

symbol	value	unit	description
h_c	18	m	canopy height
LAI		m ² m ⁻²	all-sided leaf area index at each layer
T		K	air temperature
q_v		kg m ⁻³	specific humidity
RH		-	relative humidity
X		-	scalar quantity
u_*		m s ⁻¹	friction velocity
u_{*g}		m s ⁻¹	friction velocity near the ground
H		W m ⁻²	sensible heat flux
LE		W m ⁻²	latent heat flux

symbol	value	unit	description
$F_{t,X}$		-	turbulent flux of X
F_t		$\mu\text{g m}^{-2} \text{s}^{-1}$	O_3 turbulent flux
K_t		$\text{m}^2 \text{s}^{-1}$	turbulent eddy diffusivity
K_h		$\text{m}^2 \text{s}^{-1}$	turbulent eddy diffusivity for heat fluxes
TKE		$\text{m}^2 \text{s}^{-2}$	turbulent kinetic energy
ε		$\text{m}^2 \text{s}^{-3}$	dissipation rate of TKE
ω		s^{-1}	specific dissipation of TKE
$C_{p,air}$	1009.0	$\text{J kg}^{-1} \text{K}^{-1}$	latent heat flux
ρ_{air}	1.205	kg m^{-3}	air density
γ_d	0.0098	K m^{-1}	lapse rate of dry air
L_v	2.256×10^6	J kg^{-1}	latent heat of vapourisation for water
C_μ	0.0436	-	closure constant in calculating K_t
A	1	$\text{m}^2 \text{m}^{-3}$	a scale factor
Q_{chem}		$\mu\text{g m}^{-3} \text{s}^{-1}$	chemical production and loss
F		$\mu\text{g m}^{-2} \text{s}^{-1}$	O_3 deposition flux
$[\text{O}_3]$		$\mu\text{g m}^{-3}$	O_3 concentration
V_d		m s^{-1}	layer-specific conductance for O_3
r_{veg}		s m^{-1}	leaf surface resistance
r_{veg1}		s m^{-1}	leaf surface resistance to the side without stomata
r_{veg2}		s m^{-1}	leaf surface resistance to the side with stomata
r_b		s m^{-1}	quasi-laminar boundary layer resistance over leaf surface
r_{ac}	0	s m^{-1}	resistance of turbulent transport from the reference height of the under-story vegetation to the soil surface
r_{bs}		s m^{-1}	soil boundary layer resistance
r_{soil}	400	s m^{-1}	soil resistance
r_{stm}		s m^{-1}	stomatal resistance
r_{stm,H_2O}		s m^{-1}	stomatal resistance for water vapour
r_{mes}	0	s m^{-1}	mesophyllic resistance
r_{cut}	10^5	s m^{-1}	cuticle resistance
r_{ws}	2000	s m^{-1}	wet skin resistance
f_{wet}		-	fraction of wet skin
D_{H_2O}	2.12×10^{-5}	$\text{m}^2 \text{s}^{-1}$	molecular diffusivity of water vapour
D_{O_3}	1.33×10^{-5}	$\text{m}^2 \text{s}^{-1}$	molecular diffusivity of O_3
κ	0.41	-	von Kármán constant

symbol	value	unit	description
δ_0		m	the height above ground where the molecular diffusivity is equal to turbulent eddy diffusivity
z_*	0.1	m	the height under which the logarithmic wind profile is assumed
Sc	1.07	-	Schmidt number for O ₃

Author contributions. Putian Zhou implemented the deposition code into SOSAA, made the simulation runs, analysed the results and ~~wrote~~ wrote the main part of this manuscript. Laurens Ganzeveld provided and developed the deposition code, suggested the concepts of manuscript structure, contributed the micrometeorology part and the discussions related to O₃ fluxes. Üllar Rannik contributed the micrometeorology part, the discussions related to O₃ flux measurements and the discussions in chemical removal processes. Luxi Zhou contributed
5 implementing the deposition code into SOSAA and configuration of simulation runs. Rosa Gierens contributed the configuration of meteorology part in SOSAA and configuration of simulation runs. Ditte Taipale contributed the discussions related to air chemistry and site description. Ivan Mammarella contributed discussions related to O₃ flux measurements. Michael Boy provided SOSAA code and the main concept and structure of this manuscript.

Acknowledgements. This work was supported by Maj ja Tor Nessling funding, the Academy of Finland (projects 1118615 and 272041),
10 CRAICC (Cryosphere-atmosphere interactions in a changing Arctic climate), eSTICC (eScience tools for investigating Climate Change in Northern High Latitudes) and FCoE (The Centre of Excellence in Atmospheric Science - From Molecular and Biological processes to The Global Climate). This work was also supported by institutional research funding (IUT20-11) of the Estonian Ministry of Education and Research, and the European Regional Development Fund (Centre of Excellence EcolChange). The authors also wish to acknowledge CSC - IT Center for Science, Finland, for computational resources.

References

- Altimir, N., Kolari, P., Tuovinen, J.-P., Vesala, T., Bäck, J., Suni, T., Kulmala, M., and Hari, P.: Foliage surface ozone deposition: a role for surface moisture?, *Biogeosciences*, 3, 209–228, 2006.
- Boy, M., Sogachev, A., Lauros, J., Zhou, L., Guenther, A., and Smolander, S.: SOSA—a new model to simulate the concentrations of organic vapours and sulphuric acid inside the ABL – Part 1: Model description and initial evaluation, *Atmos. Chem. Phys.*, 11, 43–51, 2011.
- Boy, M., Mogensen, D., Smolander, S., Zhou, L., Nieminen, T., Paasonen, P., Plass-Dülmer, C., Sipilä, M., Petäjä, T., Mauldin, L., Berresheim, H., and Kulmala, M.: Oxidation of SO₂ by stabilized Criegee intermediate (sCI) radicals as a crucial source for atmospheric sulfuric acid concentrations, *Atmospheric Chemistry and Physics*, 13, 3865–3879, doi:10.5194/acp-13-3865-2013, <http://www.atmos-chem-phys.net/13/3865/2013/>, 2013.
- 10 Bäck, J., Aalto, J., Henriksson, M., Hakola, H., He, Q., and Boy, M.: Chemodiversity of a Scots pine stand and implications for terpene air concentrations, *Biogeosciences*, 9, 689–702, 2012.
- Caird, M. A., Richards, J. H., and Donovan, L. A.: Nighttime Stomatal Conductance and Transpiration in C₃ and C₄ Plants, *Plant Physiology*, 143, 4–10, 2007.
- Dee, D. P., Uppala, S. M., Simmons, A. J., Berrisford, P., Poli, P., Kobayashi, S., Andrae, U., Balmaseda, M. A., Balsamo, G., Bauer, P., Bechtold, P., Beljaars, A. C. M., van de Berg, L., Bidlot, J., Bormann, N., Delsol, C., Dragani, R., Fuentes, M., Geer, A. J., Haimberger, L., Healy, S. B., Hersbach, H., Hólm, E. V., Isaksen, I., Kållberg, P., Köhler, M., Matricardi, M., McNally, A. P., Monge-Sanz, B. M., Morcrette, J.-J., Park, B.-K., Peubey, C., de Rosnay, P., Tavolato, C., Thépaut, J.-N., and Vitart, F.: The ERA-Interim reanalysis: configuration and performance of the data assimilation system, *Quarterly Journal of the Royal Meteorological Society*, 137, 553–597, doi:10.1002/qj.828, <http://dx.doi.org/10.1002/qj.828>, 2011.
- 15 Fares, S., McKay, M., Holzinger, R., and Goldstein, A. H.: Ozone fluxes in a *Pinus ponderosa* ecosystem are dominated by non-stomatal processes: Evidence from long-term continuous measurements, *Agricultural and Forest Meteorology*, 150, 420–431, 2010.
- Felzer, B. S., Cronin, T., Reilly, J. M., Melillo, J. M., and Wang, X.: Impacts of ozone on trees and crops, *Comptes Rendus Geoscience*, 339, 784–798, 2007.
- Ganzeveld, L. and Lelieveld, J.: Dry deposition parameterization in a chemistry general circulation model and its influence on the distribution of reactive trace gases, *J. Geophys. Res.*, 100, 20 999–21 012, 1995.
- 25 Ganzeveld, L., Lelieveld, J., and Roelofs, G.-J.: A dry deposition parameterization for sulfur oxides in a chemistry and general circulation model, *Journal of Geophysical Research: Atmospheres*, 103, 5679–5694, doi:10.1029/97JD03077, <http://dx.doi.org/10.1029/97JD03077>, 1998.
- Ganzeveld, L., Bouwman, L., Stehfest, E., van Vuuren, D. P., Eickhout, B., and Lelieveld, J.: Impact of future land use and land cover changes on atmospheric chemistry-climate interactions, *Journal of Geophysical Research: Atmospheres*, 115, n/a–n/a, doi:10.1029/2010JD014041, <http://dx.doi.org/10.1029/2010JD014041>, d23301, 2010.
- 30 Ganzeveld, L. N., Lelieveld, J., Dentener, F. J., Krol, M. C., Bouwman, A. J., and Roelofs, G.-J.: Global soil-biogenic NO_x emissions and the role of canopy processes, *Journal of Geophysical Research*, 107, ACH 9–1–ACH 9–17, doi:10.1029/2001JD001289, <http://dx.doi.org/10.1029/2001JD001289>, 2002a.
- 35 Ganzeveld, L. N., Lelieveld, J., Dentener, F. J., Krol, M. C., and Roelofs, G.-J.: Atmosphere-biosphere trace gas exchanges simulated with a single-column model, *Journal of Geophysical Research*, 107, ACH 8–1–ACH 8–21, doi:10.1029/2001JD000684, <http://dx.doi.org/10.1029/2001JD000684>, 2002b.

- Gierens, R. T., Laakso, L., Mogensen, D., Vakkari, V., Beukes, J. P., Van Zyl, P. G., Hakola, H., Guenther, A., Pienaar, J. J., and Boy, M.: Modelling new particle formation events in the South African savannah, *South African Journal of Science*, doi:10.1590/sajs.2014/20130108, 2014.
- Goldstein, A. H., McKay, M., Kurpius, M. R., Schade, G. W., Lee, A., Holzinger, R., and Rasmussen, R. A.: Forest thinning experiment confirms ozone deposition to forest canopy is dominated by reaction with biogenic VOCs, *Geophysical Research Letters*, 31, n/a–n/a, doi:10.1029/2004GL021259, <http://dx.doi.org/10.1029/2004GL021259>, 122106, 2004.
- Guenther, A. B., Karl, T., Harley, P., Wiedinmyer, C., Palmer, P. I., and Geron, C.: Estimates of global terrestrial isoprene emissions using MEGAN(Model of Emissions of Gases and Aerosols from Nature), *Atmos. Chem. Phys.*, 6, 3181–3210, 2006.
- Hardacre, C., Wild, O., and Emberson, L.: An evaluation of ozone dry deposition in global scale chemistry climate models, *Atmos. Chem. Phys.*, 15, 6419–6436, 2015.
- Hari, P. and Kulmala, M.: Station for Measuring Ecosystem-Atmosphere Relations (SMEAR II), *Boreal Environ. Res.*, 10, 315–322, 2005.
- Junninen, H., Lauri, A., Keronen, P., Aalto, P., Hiltunen, V., Hari, P., and Kulmala, M.: Smart-SMEAR: on-line data exploration and visualization tool for SMEAR stations, *Boreal Environment Research*, 14, 447–457, 2009.
- Kampa, M. and Castanas, E.: Human health effects of air pollution, *Environmental Pollution*, 151, 362–367, 2008.
- Keronen, P., Reissell, A., Rannik, Ü., Pohja, T., Siivola, E., Hiltunen, V., Hari, P., Kulmala, M., and Vesala, T.: Ozone flux measurements over a Scots pine forest using eddy covariance method: performance evaluation and comparison with flux-profile method, *Boreal Environ. Res.*, 8, 425–443, 2003.
- Kolari, P., Pumpanen, J., Kulmala, L., Ilvesniemi, H., Nikinmaa, E., Grönholm, T., and Hari, P.: Forest floor vegetation plays an important role in photosynthetic production of boreal forests, *Forest Ecology and Management*, 221, 241–248, 2006.
- Kolari, P., Lappalainen, H. K., Hänninen, H., and Hari, P.: Relationship between temperature and the seasonal course of photosynthesis in Scots pine at northern timberline and in southern boreal zone, *Tellus B*, 59, 542–552, doi:10.1111/j.1600-0889.2007.00262.x, <http://dx.doi.org/10.1111/j.1600-0889.2007.00262.x>, 2007.
- Korhonen, H., Lehtinen, K. E. J., and Kulmala, M.: Multicomponent aerosol dynamics model UHMA: model development and validation, *Atmospheric Chemistry and Physics*, 4, 757–771, doi:10.5194/acp-4-757-2004, <http://www.atmos-chem-phys.net/4/757/2004/>, 2004.
- Kulmala, L., Launiainen, S., Pumpanen, J., Lankreijer, H., Lindroth, A., Hari, P., and Vesala, T.: H₂O and CO₂ fluxes at the floor of a boreal pine forest, *Tellus B*, 60, 167–178, doi:10.1111/j.1600-0889.2007.00327.x, <http://dx.doi.org/10.1111/j.1600-0889.2007.00327.x>, 2008.
- Kurpius, M. R. and Goldstein, A. H.: Gas-phase chemistry dominates O₃ loss to a forest, implying a source of aerosols and hydroxyl radicals to the atmosphere, *Geophysical Research Letters*, 30, n/a–n/a, doi:10.1029/2002GL016785, <http://dx.doi.org/10.1029/2002GL016785>, 1371, 2003.
- Kurtén, T., Zhou, L., Makkonen, R., Merikanto, J., Räsänen, P., Boy, M., Richards, N., Rap, A., Smolander, S., Sogachev, A., Guenther, A., Mann, G. W., Carslaw, K., and Kulmala, M.: Large methane releases lead to strong aerosol forcing and reduced cloudiness, *Atmospheric Chemistry and Physics*, 11, 6961–6969, doi:10.5194/acp-11-6961-2011, <http://www.atmos-chem-phys.net/11/6961/2011/>, 2011.
- Lamaud, E., Carrara, A., Brunet, Y., Lopez, A., and Druilhet, A.: Ozone fluxes above and within a pine forest canopy in dry and wet conditions, *Atmospheric Environment*, 36, 77–88, 2002.
- Lammel, G.: Formation of nitrous acid: parameterisation and comparison with observations, Tech. Rep. REPORT No. 286, Max-Planck-Institut für Meteorologie, 1999.
- Launiainen, S., Katul, G. G., Grönholm, T., and Vesala, T.: Partitioning ozone fluxes between canopy and forest floor by measurements and a multi-layer model, *Agricultural and Forest Meteorology*, 173, 85–99, 2013.

- Mammarella, I., Peltola, O., Nordbo, A., Järvi, L., and Rannik, Ü.: Quantifying the uncertainty of eddy covariance fluxes due to the use of different software packages and combinations of processing steps in two contrasting ecosystems, *Atmospheric Measurement Techniques*, 9, 4915–4933, doi:doi:10.5194/amt-9-4915-2016, 2016.
- Massman, W. J.: Toward an ozone standard to protect vegetation based on effective dose: a review of deposition resistances and a possible
5 metric, *Atmospheric Environment*, 38, 2323–2337, 2004.
- Meyers, T. P.: The sensitivity of modeled SO₂ fluxes and profiles to stomatal and boundary layer resistances, *Water, Air, and Soil Pollution*, 35, 261–278, doi:10.1007/BF00290935, <http://dx.doi.org/10.1007/BF00290935>, 1987.
- Mogensen, D., Smolander, S., Sogachev, A., Zhou, L., Sinha, V., Guenther, A., Williams, J., Nieminen, T., Kajos, M. K., Rinne, J., Kulmala, M., and Boy, M.: Modelling atmospheric OH-reactivity in a boreal forest ecosystem, *Atmos. Chem. Phys.*, 11, 9709–9719, 2011.
- 10 Mogensen, D., Gierens, R., Crowley, J. N., Keronen, P., Smolander, S., Sogachev, A., Nölscher, A. C., Zhou, L., Kulmala, M., Tang, M. J., Williams, J., and Boy, M.: Simulations of atmospheric OH, O₃ and NO₃ reactivities within and above the boreal forest, *Atmos. Chem. Phys.*, 15, 3909–3932, 2015.
- Nemitz, E., Sutton, M. A., Schjoerring, J. K., Husted, S., and Paul, W. G.: Resistance modelling of ammonia exchange over oilseed rape, *Agricultural and Forest Meteorology*, 105, 405–425, 2000.
- 15 Rannik, Ü., Kolari, P., Vesala, T., and Hari, P.: Uncertainties in measurement and modelling of net ecosystem exchange of a forest, *Agricultural and Forest Meteorology*, 138, 244–257, 2006.
- Rannik, U., Mammarella, I., Keronen, P., and Vesala, T.: Vertical advection and nocturnal deposition of ozone over a boreal pine forest, *Atmospheric Chemistry and Physics*, 9, 2089–2095, doi:10.5194/acp-9-2089-2009, <http://www.atmos-chem-phys.net/9/2089/2009/>, 2009.
- Rannik, U., Altimir, N., Mammarella, I., Bäck, J., Rinne, J., Ruuskanen, T. M., Hari, P., Vesala, T., and Kulmala, M.: Ozone deposition into a
20 boreal forest over a decade of observations: evaluating deposition partitioning and driving variables, *Atmospheric Chemistry and Physics*, 12, 12 165–12 182, doi:10.5194/acp-12-12165-2012, <http://www.atmos-chem-phys.net/12/12165/2012/>, 2012.
- Rinne, J., Bäck, J., and Hakola, H.: Biogenic volatile organic compound emissions from the Eurasian taiga: current knowledge and future directions, *Boreal Environment Research*, 14, 807–826, 2009.
- Ruckstuhl, K. E., Johnson, E. A., and Miyaniishi, K.: Introduction. The boreal forest and global change, *Philosophical Transactions of the
25 Royal Society of London B: Biological Sciences*, 363, 2243–2247, doi:10.1098/rstb.2007.2196, <http://rstb.royalsocietypublishing.org/content/363/1501/2243>, 2008.
- Seok, B., Helmig, D., Ganzeveld, L., Williams, M. W., and Vogel, C. S.: Dynamics of nitrogen oxides and ozone above and within a mixed hardwood forest in northern Michigan, *Atmospheric Chemistry and Physics*, 13, 7301–7320, doi:10.5194/acp-13-7301-2013, <http://www.atmos-chem-phys.net/13/7301/2013/>, 2013.
- 30 Smolander, S., He, Q., Mogensen, D., Zhou, L., Bäck, J., Ruuskanen, T., Noe, S., Guenther, A., Aaltonen, H., Kulmala, M., and Boy, M.: Comparing three vegetation monoterpene emission models to measured gas concentrations with a model of meteorology, air chemistry and chemical transport, *Biogeosciences*, 11, 5425–5443, 2014.
- Sogachev, A.: A note on two-equation closure modelling of canopy flow, *Boundary-Layer Meteorol.*, 130, 423–435, 2009.
- Sogachev, A., Menzhulin, G., Heimann, M., and Lloyd, J.: A simple three dimensional canopy – planetary boundary layer simulation model
35 for scalar concentrations and fluxes., *Tellus*, 54B, 784–819, 2002.
- Stocker, T. F., Qin, D., Plattner, G.-K., Tignor, M., Allen, S. K., Boschung, J., Nauels, A., Xia, Y., Bex, V., and Midgley, P. M.: IPCC, 2013: Climate Change 2013: The Physical Science Basis. Contribution of Working Group I to the Fifth Assessment Report of the Intergovernmental Panel on Climate Change, Cambridge University Press, Cambridge, United Kingdom and New York, NY, USA, 2013.

- Wesely, M. L.: Parameterization of surface resistances to gaseous dry deposition in regional-scale numerical models, *Atmos. Env.*, 23, 1293–1304, 1989.
- Williams, J., Crowley, J., Fischer, H., Harder, H., Martinez, M., Petäjä, T., Rinne, J., Bäck, J., Boy, M., Dal Maso, M., Hakala, J., Kajos, M., Keronen, P., Rantala, P., Aalto, J., Aaltonen, H., Paatero, J., Vesala, T., Hakola, H., Levula, J., Pohja, T., Herrmann, F., Auld, J., Mesarchaki, E., Song, W., Yassaa, N., Nölscher, A., Johnson, A. M., Custer, T., Sinha, V., Thieser, J., Pouvesle, N., Taraborrelli, D., Tang, M. J., Bozem, H., Hosaynali-Beygi, Z., Axinte, R., Oswald, R., Novelli, A., Kubistin, D., Hens, K., Javed, U., Trawny, K., Breitenberger, C., Hidalgo, P. J., Ebben, C. J., Geiger, F. M., Corrigan, A. L., Russell, L. M., Ouwersloot, H. G., Vilà-Guerau de Arellano, J., Ganzeveld, L., Vogel, A., Beck, M., Bayerle, A., Kampf, C. J., Bertelmann, M., Köllner, F., Hoffmann, T., Valverde, J., González, D., Riekkola, M.-L., Kulmala, M., and Lelieveld, J.: The summertime Boreal forest field measurement intensive (HUMPPA-COPEC-2010): an overview of meteorological and chemical influences, *Atmospheric Chemistry and Physics*, 11, 10 599–10 618, doi:10.5194/acp-11-10599-2011, <http://www.atmos-chem-phys.net/11/10599/2011/>, 2011.
- Wolfe, G. M. and Thornton, J. A.: The Chemistry of Atmosphere-Forest Exchange (CAFE) Model - Part 1: Model description and characterization, *Atmospheric Chemistry and Physics*, 11, 77–101, doi:10.5194/acp-11-77-2011, <http://www.atmos-chem-phys.net/11/77/2011/>, 2011.
- Wolfe, G. M., Thornton, J. A., McKay, M., and Goldstein, A. H.: Forest-atmosphere exchange of ozone: sensitivity to very reactive biogenic VOC emissions and implications for in-canopy photochemistry, *Atmospheric Chemistry and Physics*, 11, 7875–7891, doi:10.5194/acp-11-7875-2011, <http://www.atmos-chem-phys.net/11/7875/2011/>, 2011.
- Wu, Y., Brashers, B., Finkelstein, P. L., and E., P. J.: A multilayer biochemical dry deposition model 1. Model formulation, *Journal of Geophysical Research: Atmospheres*, 108, doi:10.1029/2002JD002306, <http://dx.doi.org/10.1029/2002JD002306>, 2003.
- Zhou, L., Nieminen, T., Mogensen, D., Smolander, S., Rusanen, A., Kulmala, M., and Boy, M.: SOSAA – a new model to simulate the concentrations of organic vapours, sulphuric acid and aerosols inside the ABL – Part 2: Aerosol dynamics and one case study at a boreal forest site, *Boreal Environment Research*, 19 (suppl. B), 237–256, 2014.
- Zhou, L., Gierens, R., Sogachev, A., Mogensen, D., Ortega, J., Smith, J. N., Harley, P. C., Prenni, A. J., Levin, E. J. T., Turnipseed, A., Rusanen, A., Smolander, S., Guenther, A. B., Kulmala, M., Karl, T., and Boy, M.: Contribution from biogenic organic compounds to particle growth during the 2010 BEACHON-ROCS campaign in a Colorado temperate needleleaf forest, *Atmospheric Chemistry and Physics*, 15, 8643–8656, doi:10.5194/acp-15-8643-2015, <http://www.atmos-chem-phys.net/15/8643/2015/>, 2015.